

DEVELOPMENT OF ANIMAL MODELS IN PEDIATRIC CANCER

by

Priyanka Dhanan

A thesis submitted to the Faculty of the University of Delaware in partial fulfillment of the requirements for the degree of Master of Science in Biological Sciences

Fall 2014

© 2014 Priyanka Dhanan
All Rights Reserved

UMI Number: 1585144

All rights reserved

INFORMATION TO ALL USERS

The quality of this reproduction is dependent upon the quality of the copy submitted.

In the unlikely event that the author did not send a complete manuscript and there are missing pages, these will be noted. Also, if material had to be removed, a note will indicate the deletion.



UMI 1585144

Published by ProQuest LLC (2015). Copyright in the Dissertation held by the Author.

Microform Edition © ProQuest LLC.

All rights reserved. This work is protected against unauthorized copying under Title 17, United States Code



ProQuest LLC.
789 East Eisenhower Parkway
P.O. Box 1346
Ann Arbor, MI 48106 - 1346

DEVELOPMENT OF ANIMAL MODELS IN PEDIATRIC CANCER

by

Priyanka Dhanan

Approved: _____
Anja Nohe, Ph.D.
Professor in charge of thesis on behalf of the Advisory Committee

Approved: _____
Robert W. Mason, Ph.D.
Professor in charge of thesis on behalf of the Advisory Committee

Approved: _____
Salil A. Lachke, Ph.D.
Professor in charge of thesis on behalf of the Advisory Committee

Approved: _____
Randall L. Duncan, Ph.D.
Chair of the Department of Biological Sciences

Approved: _____
George H. Watson, Ph.D.
Dean of the College of Arts & Sciences

Approved: _____
James G. Richards, Ph.D.
Vice Provost for Graduate and Professional Education

ACKNOWLEDGMENTS

I have had the privilege to work with two wonderful advisors at different points of my project. First and foremost I would like to thank my advisor, Dr Robert W Mason, for all the support throughout my graduate program without whom this achievement would not be accomplished. I am extremely grateful for all the guidance and patience he has shown through this important phase of my life. I would also like to thank my co-advisor, Dr Sonali Barwe, without whom none of this would have been possible. I am very thankful for giving me an opportunity to be a part of your wonderful lab.

I would like to thank my committee members, Dr. Anja Nohe and Dr. Salil Lachke for their guidance and support that has shaped my project to where it is today. I would like to thank all my lab members of both labs for their advice and support. A very special thanks to Guizhen Lu who trained me on various cell biology techniques that were vital for the successful completion of my project. She has been an amazing person to work with and I could not have asked for a better person to introduce me to the lab by giving me my initial training .I would also like to thank Lisa Glazewski, Mehrnoosh Soori and Bruce Korant for their guidance and moral support .A very special thanks to Anilkumar.G for working with me as a great team and helping me with all the animal work.

A special thank you goes out to the SNERPS, particularly David Wu, Yu Peng, Sona Balasubramaniam, and Pratima Patil who has given me advice and much needed assistance throughout my project. I would to give a special thanks to Miho Maeda for helping me plan my graduate course work. I would like to thank all the research assistants and post-docs in Rockland I at Nemours AI duPont Hospital for Children for their support and guidance. Furthermore, my time at both UD and Nemours would not have been as smooth if it wasn't for the help of Betty Cowgill and for that I am very thankful.

This dream was made possible by one person to whom I am eternally indebted- my wonderful husband Vinu Krishnan. Thank you for being my pillar of strength and support throughout this journey. Last but not least, I would like to thank my wonderful family for their unconditional love and encouragement even if they are half way across the globe.

TABLE OF CONTENTS

LIST OF FIGURES	ix
LIST OF TABLES	xi
ABSTRACT	xii
SECTION 1: NEUROBLASTOMA.....	1
Chapter	
1 INTRODUCTION	2
1.1 Neuroblastoma.....	2
1.2 Incidence Rates of Neuroblastoma.....	3
1.3 The International Neuroblastoma Staging System	4
1.4 Current Therapies for Neuroblastoma	6
1.5 Biology of Cathepsins	8
1.6 Role of Cathepsins in Cancer	8
1.7 Role of Cathepsins in the Development of the Nervous System.....	9
1.8 Effect of Inhibition of Cathepsins B and L by FYAD on Neuroblastoma Cells	10
1.9 Autophagy	11
1.10 Role of Autophagy in Cancer	12
1.11 Hypothesis	14
2 MATERIALS AND METHODS.....	15
2.1 Cell Lines and Culture.....	15
2.2 Cathepsin Inhibitors.....	15
2.3 Quantitative Assessments of Cell Viability.....	16
2.4 Quantitative Assessments of Enzyme Activity	16
2.5 Western Blot Analysis	17
2.6 Xenograft Model of Neuroblastoma.....	17
2.7 Small Interfering RNA Transfection for Cathepsin B Knockdown	19
3 RESULTS	20

3.1	Analysis of Enzyme Activity After Addition of Inhibitors to Neuroblastoma Cells	20
3.2	Dose-Dependent Effect of Inhibitors on Neuroblastoma Cell Viability ..	27
3.3	Accumulation of Cleaved LC-3 in Inhibitor Treated Neuroblastoma Cells.....	29
3.4	Cathepsin B Knockdown by Small Interfering RNA(siRNA) Transfection.....	30
3.5	Cathepsin B and L Knockdown by Combining Small Interfering RNA(siRNA) Transfection and Cathepsin B and L Inhibitor FYAD	32
3.6	<i>In vivo</i> Characterization of the Effects of L264, Reversible Cathepsin B Inhibitor	33
3.7	Levels of Cathepsin B Protein in Tumors During and After Treatment with L264	36
3.8	Arrest of Tumor Growth In Vivo by K11777,Irreversible Cathepsin B Inhibitor	38
3.9	Effects on Enzyme Activity of Various Tissues due to Cathepsin Inhibition by Drug K11777	39
4	DISCUSSION.....	41
4.1	Efficacy of Compounds to Induce Neuroblastoma Cell Death Depends on the Inhibition of Cathepsin B and L Enzymes.	41
4.2	Autophagy is Related to the Cell Death Caused by the Treatment of the Inhibitors.....	43
4.3	Effects of Reversible Inhibitor L264 on Neuroblastoma Cell Growth In Vivo.....	44
4.4	Cathepsin Inhibition by Irreversible Inhibitor K11777 Reduces Neuroblastoma Cell Growth.....	45
4.5	Inhibitors for Cathepsins B and L for Potential Clinical Use.....	45
	REFERENCES	47
	SECTION 2: LEUKEMIA.....	52
5	INTRODUCTION	53
5.1	Leukemia	53
5.2	Types of Leukemia	55
5.3	Incidence Rates of Leukemia	56
5.4	Current Therapies for Leukemia	57
5.5	Preclinical Mouse Models of Leukemia.....	59
6	MATERIALS AND METHODS.....	62

6.1	Cell Lines and Culture.....	62
6.2	Leukemia Cells from Patient Samples	62
6.3	Engraftment of Human Leukemia Cells into NSG B2m Mice.....	63
6.4	Monitoring of Leukemic Cells After Engraftment and Flow Cytometric Analysis	64
7	RESULTS	67
7.1	Engraftment of Primary Childhood ALL Cells	67
7.2	Analysis of Engraftment and Progression of ALL Cells.....	68
7.3	Analysis of Leukemic Distribution in Other Organs.....	69
7.4	Enlarged Leukemic Spleen when compared to Normal Spleen	70
7.5	Leukemia Progression in the Mouse Model	70
7.6	Serial Transplantation of Leukemic Cells in NSG-B2m Mice.....	72
8	DISCUSSION.....	74
	REFERENCES	78
Appendix		
A	IACUC LETTER OF APPROVAL.....	82
B	IACUC LETTER OF APPROVAL.....	83
C	IRB LETTER OF APPROVAL.....	84

LIST OF FIGURES

Figure 3.1: In the above figure, SKNSH cells were not treated with inhibitors and were used as control to detect the cathepsin B + L enzyme activity.	22
Figure 3.2: Enzyme activity of cathepsin B when treated with irreversible inhibitors FYAD and LHVS.	23
Figure 3.3: Enzyme activity of cathepsin B when treated with reversible inhibitors VBY-825(cathepsin B, L and S inhibitor) and VBY-754 (cathepsin B, L and S inhibitor).	24
Figure 3.4: Enzyme activity of cathepsin B when treated with reversible inhibitors VBY-129 (cathepsin S inhibitor) and VBY-376 (cathepsin B inhibitor).	25
Figure 3.5: Comparative representation of enzyme activity of cathepsins B and L when treated with various reversible and irreversible inhibitors on SKNSH cells.	26
Figure 3.6: Concentration effect of cathepsin inhibitors on neuroblastoma cell survival.	29
Figure 3.7: Accumulation of LC-3 in inhibitor treated neuroblastoma cells.	30
Figure 3.8: Cathepsin B knockdown by small interfering RNA(siRNA) Transfection.	31
Figure 3.9: Cathepsin B knockdown by combining small interfering RNA(siRNA) Transfection and cathepsin inhibitor FYAD.	32
Figure 3.10: <i>In vivo</i> characterization of the effects of L264, reversible cathepsin B inhibitor.	35
Figure 3.11: Cathepsin B protein levels in tumors during and after treatment with L264.	37
Figure 3.12: Effects of K11777 on tumor growth <i>in vivo</i> . 10 ⁷ SK-N-SH cells were injected subcutaneously into hairless/SCID mice.	38

Figure 3.13: Effects of K11777 on cathepsin enzyme activity <i>in vivo</i>	40
Figure 5.1: Schematic representation of normal blood cell development.....	54
Figure 5.2: Proportion of new cases for the types of leukemia in adults and children 2014	56
Figure 6.1: Sub-mandibular bleeding in mice.....	64
Figure 6.2: Intravenous transfer of ALL cells.....	66
Figure 7.1: Engraftment and progression of human ALL cells in peripheral blood. .	69
Figure 7.2: Engraftment and progression of human leukocytes measured in spleen and bone marrow.....	69
Figure 7.3: Comparison of a leukemic spleen to a normal spleen.	70
Figure 7.4: a) normal mouse b) mouse infected with leukemic cells c) Graph representing leukemic progression d) Leukemic progression shown in flow cytometry.....	72
Figure 7.5: a) Ficoll Gradient showing the separated layer of leukocytes from a spleen sample. b) Graphical representation showing similar engraftment rates in serial transplantation.....	73

LIST OF TABLES

Table 5-1: Number of new leukemia cases in the United States 2014	57
Table 7-1: Patient samples used in development of xenograft mouse model for leukemia	67

ABSTRACT

The study was designed to develop xenograft mouse model in pediatric cancers with focus upon neuroblastoma - the most common form of solid tumors in childhood cancer and leukemia- the most prevalent form of pediatric cancer. The thesis consists of two sections- Section1 includes testing and validating the therapeutic efficacies of novel compounds in preclinical models of neuroblastoma and Section 2 details the development of an experimental animal model for childhood leukemia. The study on neuroblastoma was designed to test a panel of reversible and irreversible inhibitors of cathepsin B and L to induce death of neuroblastoma cells. Efficacy of the compounds depends on their ability to inhibit enzyme activity of cathepsins B and L. Five compounds that differ in mode and rate of inhibition of enzymes were tested to evaluate their ability to cause neuroblastoma cell death. Cysteine protease inhibitors that could not achieve at least 90% inhibition of enzyme activity *in vitro* failed to control neuroblastoma tumor growth *in vivo*. Treatment with inhibitors caused an increase in markers of cell stress and induced expression of autophagic markers LC3-II indicating that apoptosis was preceded by autophagy. The levels of LC3-II were highest for cells treated with irreversible inhibitors than reversible inhibitors. In contrast to irreversible inhibitors which markedly impaired tumor growth *in vivo*; reversible inhibitors failed to induce neuroblastoma cell death and did not control tumor growth. These results illustrated that irreversible inhibitors are better candidates for control of tumor growth and bring about death of neuroblastoma cells. It is

concluded that development of drugs to target these two proteases may provide a novel approach in treating neuroblastoma.

Section 2 includes the study designed to create human leukemia xenografts in immunodeficient mice. This would provide an important tool to understand various aspects of leukemia disease origin and subsequent progression while identifying and evaluating novel therapeutic strategies. The disease models developed in this study used both cell lines and primary human acute lymphoblastic leukemia cells to create xenografts that recapitulate clinical features of the disease. Similar to the human environment, the injected leukemia cells in the mouse are exposed to both favorable and unfavorable conditions for engraftment. Cells harvested from the spleens of engrafted mice readily initiated leukemia in secondary and tertiary recipients. High-level infiltration of bone marrow, spleen, and liver was observed. The immunophenotypes of xenografts were essentially unaltered compared with that of the patient sample. In this study we hypothesized that the biologic characteristics of childhood ALL xenografts accurately reflected the clinical disease. The animal disease models developed in this study provides powerful experimental tools to prioritize new therapeutic strategies for future clinical trials.

SECTION 1: NEUROBLASTOMA

Chapter 1

INTRODUCTION

1.1 Neuroblastoma

Neuroblastoma develops from neuroblast stem cells of the neural crest. Normally, these cells divide and after a migratory phase they differentiate into cells of the peripheral nervous system or into adrenal medulla cells in the center of the adrenal gland. In humans, most of this developmental process occurs prior to birth. Neuroblasts that fail to mature and continue to divide lead to neuroblastoma, a solid cancerous tumor that becomes apparent in infants and children aged less than 5 years. Neuroblastoma can originate in the nerve tissue near the spine in the neck, chest, abdomen, or pelvis, and more often in the adrenal glands. Thus it can be considered to be a developmental defect caused by failure of neural crest cells to differentiate into cells of the adrenal glands and peripheral nervous system. Sometimes it can also be detected in a prenatal (before birth) ultrasound scan. Most often, however, neuroblastoma is detected after the cancer has spread to other parts of the body, such as the lymph nodes, liver, lungs, bones, and bone marrow [reviewed in Maris 2010, van Noesel et al. 2004, Volchenbum et al 2009]. The clinical presentation is highly variable, ranging from a mass that causes no symptoms to a primary tumor that causes critical illness as a result of local invasion, widely disseminated disease, or both.

1.2 Incidence Rates of Neuroblastoma

Neuroblastoma is the most common form of extra cranial solid tumor in children. More than 650 cases are diagnosed each year in North America. The prevalence is about 1 case per 7,000 live births and its incidence is about 10 cases per 1 million every year in children younger than 15 years of age (London W.B et al.2005) 37% are diagnosed as infants, and 90% are younger than 5 years, with a median age at diagnosis of 19 months. Neuroblastoma accounts for 6% of all childhood cancers in the United States. It is the most commonly occurring cancer in babies younger than one and the third most common tumor in children. The five-year survival rate for children with low-risk neuroblastoma is higher than 95% (Cancer Facts & Figures 2013). For children with intermediate-risk neuroblastoma, the survival rate is 80% to 90%. However, for children with high-risk neuroblastoma, the survival rate is only 30 to 50%.

1.3 The International Neuroblastoma Staging System

Stage/Prognostic Group	Description
Stage 1	Localized tumor with complete gross excision, with or without microscopic residual disease; representative ipsilateral lymph nodes negative for tumor microscopically (nodes attached to and removed with the primary tumor may be positive).
Stage 2A	Localized tumor with incomplete gross excision; representative ipsilateral nonadherent lymph nodes negative for tumor microscopically.
Stage 2B	Localized tumor with or without complete gross excision, with ipsilateral nonadherent lymph nodes positive for tumor. Enlarged contralateral lymph nodes must be negative microscopically

<p>Stage 3</p>	<p>Unresectable unilateral tumor infiltrating across the midline, with or without regional lymph node involvement; or localized unilateral tumor with contralateral regional lymph node involvement; or midline tumor with bilateral extension by infiltration (unresectable) or by lymph node involvement. The midline is defined as the vertebral column. Tumors originating on one side and crossing the midline must infiltrate to or beyond the opposite side of the vertebral column.</p>
<p>Stage 4</p>	<p>Any primary tumor with dissemination to distant lymph nodes, bone, bone marrow, liver, skin, and/or other organs, except as defined for stage 4S.</p>

<p>Stage 4S</p>	<p>Localized primary tumor, as defined for stage 1, 2A, or 2B, with dissemination limited to skin, liver, and/or bone marrow (by definition limited to infants younger than 12 months).[Taggart et al. 2011] Marrow involvement should be minimal (i.e., <10% of total nucleated cells identified as malignant by bone biopsy or by bone marrow aspirate). More extensive bone marrow involvement would be considered stage 4 disease. The results of the mIBG scan, if performed, should be negative for disease in the bone marrow.</p>
<p><i>mIBG = metaiodobenzylguanidine,</i> http://www.cancer.gov/cancertopics/pdq/treatment/neuroblastoma/HealthProfessional/Table3</p>	

1.4 Current Therapies for Neuroblastoma

Treatment for neuroblastoma generally depends on various factors including size and location of the tumor, degree of metastasis, the risk classification, possible side effects, family preferences, and the child’s overall health. In most cases, the treatment is tailored according to the risk group the patient is assigned to and may require a combination of therapies. The neuroblastoma is often not detected until after

the cancer has spread. If the tumor has not spread, surgery alone may be able to remove the entire tumor. If the tumor cannot be completely removed, the patient may undergo radiation therapy or chemotherapy to kill the remaining cancer cells in the body. Chemotherapy drugs kill cancer cells by inhibiting their ability to grow and divide. The drugs are often delivered systemically via the bloodstream to reach cancer cells throughout the body. Chemotherapy may be used as the primary treatment for neuroblastoma, or it may be given before surgery to shrink the tumor or after surgery to kill any remaining cancer cells. Some of the most commonly used chemotherapeutic agents are Carboplatin, Cyclophosphamide and Doxorubicin. Radiation therapy is also recommended in some cases where high-energy x-rays or other particles are applied to destroy cancer cells. Side-effects of general cytotoxic chemotherapy are particularly severe for children, and the success rate for treatment of patients with advanced stages of neuroblastoma remains poor. Furthermore, these therapies that were originally designed to treat adult cancers are particularly toxic to growing children and can cause life-long side effects and even lead to the development of additional cancers. It is for these reasons that alternative approaches of treatment are required. In this study, we hypothesized that implementation of compounds from therapeutic studies that are already in clinical trials for treatment of other diseases, such as Osteoporosis (Perez-Castrillon JL et al 2010) and Chagas disease (Mohammed Sajid et al 2011), will provide drugs with better pharmacokinetics which may enhance the development of a new treatment for neuroblastoma.

1.5 Biology of Cathepsins

Cathepsins are the primary enzymes responsible for mammalian protein degradation in the lysosome. There are several enzymes involved in lysosomal proteolysis which are active only in the right environment. In the lysosomes, proteins are degraded to smaller peptides and amino acids by combined actions of endo- and exo-peptidases. Almost all the endolysosomal proteases are called cathepsins. There are 11 human cathepsin cysteine proteases, cathepsins B,H,L,S,C,K,O,F,V,X and W and two aspartic proteases, cathepsins D and E. The cysteine cathepsins are structurally related to the plant enzyme, papain. Cathepsins are synthesized as inactive pre-pro-enzymes having a signal peptide and an N terminal pro-peptide. The signal peptide delivers the cathepsin precursor into the lumen of the rough endoplasmic reticulum and is co-translationally removed (Kornfeld S 1992). The pro region is required for folding of the nascent cathepsin and inhibits proteolytic activity of the enzyme by blocking the active site. The three dimensional structure of the pro-enzyme is stable at neutral pH, maintaining the precursor in its inactive state. The procathepsin undergoes asparagine-linked glycosylation and carbohydrate processing in the Golgi. As the pH drops during transport to the late endosomes the pro cathepsins become less stable and are processed into active proteases.

1.6 Role of Cathepsins in Cancer

As described above, in normal cells cysteine cathepsins are usually localized within the lysosome or other intracellular compartments, and their main function is to aid in protein degradation and processing. In some human and mouse cancers increased expression and activity levels of cysteine cathepsins have been reported. Under some pathological conditions, these cathepsins get translocated from the

intracellular compartments to the cell surface and are sometimes even secreted by tumor cells. The enzymes can then degrade ECM components and basement membranes, thereby assisting in tumor cell invasion and metastasis (Sloane et al., 1994). Other studies have shown that elevated levels of tumor cathepsins can exceed levels of extracellular cathepsin inhibitors (cystatins) leading to uncontrolled proteolysis of the ECM. Cathepsins were also found to play a major role in angiogenesis. In order for the tumor to increase in size they need to be fed on by the formation of new blood vessels. It has been shown that cathepsin B degrades ECM, enabling migration of endothelial cells. It also aids in tumor associated angiogenesis by activating TGF- β , a critical factor for the development of the vascular structure. Detection of these proteins in extracellular fluids may extend their application to diagnosis (Advances in Enzyme Regulation 2001).

1.7 Role of Cathepsins in the Development of the Nervous System

Cathepsins play a vital role in the development of the nervous system. For example, deficiency in cathepsin K has been shown to have a multiple-level impact on brain development and metabolism. Studies have shown that the metabolism and structure of non-neuronal cells were significantly disconcerted in the CNS of cathepsin K knockdown animals (S Dauth et al 2011). The analysis of neuronal markers demonstrated that the architecture of the neuronal layers was affected by cathepsin K deficiency in particular in the hippocampus, a region of the CNS known for its importance in the regulation of anxiety and memory. The highest specific activity of cathepsin K has been observed within this region of the brain. In the present study, the focus is on the effects of cathepsins B and L in inducing neuroblastoma cell death.

Mice that are deficient in both cathepsin B and L exhibit extensive neuron death in the cerebral cortex and in the cerebral Purkinje and granule cell layers and eventually develop a pronounced brain atrophy. Most of the animals that are deficient in both the enzymes die during the weaning period even if they are carefully nursed as the neurons of these animals develop a lysosomal storage disorder. Results from all the previous studies clearly indicate that cathepsin B and L play essential roles during postnatal maturation and in maintaining the integrity of the central nervous system in mice (Sonja Stahl et al 2007).

1.8 Effect of Inhibition of Cathepsins B and L by FYAD on Neuroblastoma Cells

Previous studies have shown that neuroblastoma cells are uniquely sensitive to inhibition of both cathepsins B and L, causing apoptotic cell death (Donna M. Cartledge et al 2012). A specific irreversible inhibitor, Fmoc-Tyr-Ala-CHN₂ (FYAD), can bind to both cathepsins B and L and cause a complete chemical knockdown of the enzymes' activities. Cellular apoptosis was not attained by partial enzyme inhibition. Previous studies in our lab have shown that more than 90% enzyme inhibition is required to affect cell growth and induce cell death. Cell death by cathepsin inhibition may be due to the accumulation of proteins that are normally degraded by the combined activity of cathepsin B and L. This was proven by electron microscopy studies which traced the accumulation of dense granules in neuroblastoma cell lines over time. Proteomic studies have also shown that cell death may be preceded by autophagy by the accretion of the marker for cell stress and autophagy ,LC3-II. [Colella et al.2010].

In summary, inhibition of cathepsins B and L may provide some insight to a potential novel therapeutic approach to treat neuroblastoma. A prime limitation of FYAD was its inability to achieve complete inhibition of the enzyme's activity in vivo and thus failed to induce cell death. In the present study, a panel of inhibitors have been tested to see their potential effects in treating neuroblastoma, both in vitro and in vivo.

1.9 Autophagy

During development and nutrient stress, in order to maintain the balance of energy sources the cells undergo a self degradative process called autophagy. This process is important to remove misfolded or aggregated proteins, clearing damaged organelles, such as mitochondria, endoplasmic reticulum and peroxisomes. In addition to all these functions autophagy promotes cellular senescence and cell surface antigen presentation, protects against genome instability and prevents necrosis. Autophagy plays a key role in diseases like cancer, neurodegeneration, cardiomyopathy, diabetes, liver disease, autoimmune diseases and infection.

Autophagy begins with formation of an isolation membrane, known as a phagophore, which expands to engulf intra-cellular cargo, such as protein aggregates, organelles and ribosomes, thereby forming a double-membrane autophagosome (Mizushima N. 2007). The autophagosome then fuses with the lysosome and promotes degradation of the autophagosomal contents by lysosomal acid hydrolases. Lysosomal permeases and transporters transfer the amino acids and other by-products of degradation back out to the cytoplasm, where they can be re-used for metabolism (Mizushima N. 2007). Hence autophagy is referred to as a 'recycling factory' by providing energy through

ATP generation and preventing cell damage by removing non-functional proteins and organelles (Danielle Glick et al 2010).

1.10 Role of Autophagy in Cancer

In cancer, autophagy can act as a tumor suppressor and a mechanism of cell survival. As a tumor suppressor it prevents the accumulation of damaged parts of the cell (proteins and organelles). The high metabolic demand during rapid proliferation of tumor cells results in increased cellular stress. Previous studies have shown that inhibition of prosurvival autophagy by genetic or pharmacological means kills tumor cells by triggering apoptotic cell death (Degenhardt K et al 2006)(Amaravadi RK et al 2007).

Other studies have shown that increased autophagy leads to cell death. The role of autophagy in cancer is very complex, various pharmacological agents have been shown to induce autophagic activity resulting in massive death of cells in some cancer types (Tsujimoto Y et al 2005). One of the major causes for chemo-resistance is decreased apoptosis. Overcoming chemo-resistance would be the breakthrough needed in development of therapies in cancer treatment. Thus, activation of autophagy in apoptosis-resistant cancers could potentially provide a way to induce cell death and obstruct malignant growth (M A Hayat). Autophagic cell death is accompanied by the formation of autophagosomes/autolysosomes without chromatin condensation (Levine B et al 2004). As cancer cells are frequently resistant to drug-mediated apoptosis after long-term chemotherapeutic treatments, the induction of autophagic cell death in apoptosis-defective or apoptosis-resistant tumor cells may provide an alternative therapeutic approach to tumor suppression (Alva AS et al 2004)

Recently, a number of clinically approved or experimental anti-tumor drugs have been shown to induce autophagy-related cell death in some malignant cells (Chang CP et al 2007, Kondo Y 2005). Targeting autophagy in cancer will aim to identify optimal strategies to alter autophagy for therapeutic advantage and also provide new opportunities for drug development (Zhineng J. Yang et al 2011)

1.11 Hypothesis

The hypothesis tested in this thesis is that irreversible inhibitors of cathepsins B and L (FYAD, LHVS and K11777) will induce neuroblastoma cell death and impair tumor growth, both in vitro and in vivo. Efficacy of irreversible inhibitors is also compared to efficacy of reversible inhibitors. A series of reversible and irreversible cathepsin inhibitors with different mechanisms and rates of inhibition were tested for their ability to inhibit growth and/or cause death of neuroblastoma cells. The most promising compounds were also tested in an animal model of neuroblastoma. The long-term goal of this research is to determine whether inhibition of Cathepsin B and Cathepsin L can provide a novel approach to treatment of neuroblastoma.

Chapter 2

MATERIALS AND METHODS

2.1 Cell Lines and Culture

Two different neuroblastoma cell lines (SK-N-SH and IMR-32 cells, from ATCC) were chosen for this study. The cell lines were cultured in MEM growth media (Mediatech Inc., Manassas, VA, USA, #10-010-CV) supplemented with 10% FBS (# 35-015-CV, Mediatech Inc. Manassas, VA), 1% sodium pyruvate (Mediatech Inc., Manassas, VA, #25-30-CI) and 1% non essential amino acids (Mediatech Inc., Manassas, VA, #25-30-CI). IMR-32 cells from more aggressive N- (neuroblastic) type tumors were cultured in 75 cm² flasks and passaged upon reaching 80-90% confluence every 3-4 days by mechanical disruption. SK-N-SH cells representing less aggressive S- (substrate-adherent) type tumors were cultured in 100 mm tissue culture plates, and passaged by treating with 0.25% trypsin (Mediatech Inc. Manassas, VA, # 25-050-CI) upon reaching 80-90% confluence every 2-4 days. Cells were kept at 37°C in a humidity saturated chamber containing 95:5; v/v air: CO₂ atmosphere.

2.2 Cathepsin Inhibitors

Fmoc-Tyr-Ala-diazomethane (FYAD), previously developed in our lab, is a specific irreversible inhibitor of cathepsins B and L , and is now available from Bachem (Torrance, CA). (3R,6 S,8R)-8-(4-Bromophenyl)-6-(2-fluoro-2-methylpropyl)-5-oxo-8-(trifluoromethyl)-1-thia- 4,7-diazacycloundec-9-yne-3-carbonitrile (U.S. patent application 12/532,652), L-264, was a gift from M. David

Percival (Merck-Frosst, Canada). N-methyl-piperazine-Phe-homo-Phe-vinylsulfone-phenyl (K11777) was generously gifted by James McKerrow (University of California, San Francisco). VBY-825 and VBY-754 are specific reversible inhibitors of cathepsins B, L and S. VBY-129 is a specific reversible inhibitor of cathepsin S and VBY-376 is specific reversible inhibitor of cathepsin B. LHVS is a specific irreversible inhibitor of cathepsins B, L and S. These inhibitors were a gift from Virobay (California).

2.3 Quantitative Assessments of Cell Viability

Cathepsin inhibitor-induced cytotoxicity was measured using the cell titer blue viability assay (Promega, Madison, WI). Neuroblastoma cells were cultured in 96-well plates. Cells seeded at 50 % confluence were incubated at 37 °C with 5% CO₂ for 24 h to allow cell attachment to plates. Inhibitors or vehicle controls were then added in serial dilutions and cells were incubated for 3 days. Media was aspirated after 3 days and cell titer blue (5 µl of 1:5 PBS diluted reagent per 100 µl media, equivalent to 1 % final concentration) was added to each well and incubated for 4 h at 37 °C. Fluorescence intensity was then measured (535/595 nm, excitation/emission).

2.4 Quantitative Assessments of Enzyme Activity

The hydrolytic activity on synthetic substrates including Z-Phe-Arg-NMec was determined according to the method of Mason et al 1985 with slight modifications. Neuroblastoma cells were cultured in 96-well plates. Cells seeded at 50 % confluence were incubated at 37 °C with 5% CO₂ for 24 h to allow cell attachment to plates. Inhibitors or vehicle controls were then added at 2 different concentration (10 µM and 20 µM). Cells were treated in replicates of 6, with 6 wells containing media with no

cells for each condition as blanks. Cells were incubated for 3 days. Media was aspirated after 3 days and activity buffer (100 nM sodium acetate, pH 5.5, 1 mM EDTA, 25 μ l 1 dithiothreitol) was added to each well and incubated for 10 min at 37 °C. The enzymatic reaction was initiated by the addition of Z-Phe-Arg-NMec substrate to a final concentration of 10 or 20 μ M. The fluorescence intensity of aminomethylcoumarin released was determined at excitation wavelength, 370 nm, and emission wavelength, 460 nm, using a luminescence spectrophotometer (Victor X4, Perkin-Elmer Ltd). Data are expressed as relative expression units.

2.5 Western Blot Analysis

Total cellular proteins were dissolved in 7 M urea, 2 M thiourea, 1 % chaps, 30 mM Tris, pH 8.5 lysis buffer. Equal amounts of protein (25 μ g/lane) were separated by SDS/PAGE electrophoresis and were transferred onto Immobilon-P PVDF membranes (Millipore, Bedford, MA). Proteins were identified by immunoblotting with the following antibodies: β -actin (A5441, Sigma, St Louis, MO), LC-3 (3868, Cell Signaling, Danvers, MA). Western blot membranes were probed with anti- β -actin antibodies as a control for protein loading. A solution consisting of 200 mM glycine, 0.1 % SDS and 1 % Tween-20 at pH 2.2 was used to strip membranes prior to re-probing with different primary antibodies.

2.6 Xenograft Model of Neuroblastoma

SCID hairless sho strain code 474 mice were injected subcutaneously with 10^7 SK-N-SH cells. The cells were resuspended in 1 ml of ice cold PBS and placed on ice. 1ml of ice cold Matrigel (BD Matrigel Basement Membrane Matrix) was added to the cells with continuous mixing. 100 μ l of suspension was injected subcutaneously into

left flank of 20 mice. Once the tumors developed , they were randomized into 2 groups. Group 1 (control) was treated with saline and Group 2 (treated) was treated with an irreversible inhibitor of cathepsins B and L, K11777 (5 mg/ml in saline). The mice were injected (100 μ l) twice daily with saline or K11777 respectively for 10 consecutive days at the site of the tumor. Tumors were measured with calipers and tumor volume calculated using a modified ellipsoid formula $1/2(\text{Length} \times \text{Width}^2)$. The experiment was terminated 20 days after initiation of treatment or when tumors in animals approached a volume of 1,000 mm^3 . Once the animals were sacrificed, the different organs- kidney, liver, spleen, brain, blood and tumors were harvested for further analysis. All animal experiments were conducted in accordance with the protocols described in the NIH Guide for the Care and Use of Animals and were approved by the Nemours Biomedical Research Institutional Laboratory Animal Care and Use Committee (IACUC).

In separate experiments, SCID hairless sho strain code 474 mice were injected subcutaneously with 10^7 SK-N-SH cells. 100 μ l of suspension was injected subcutaneously into left flank of 16 mice. Once the tumors developed , they were randomized into 2 groups. Group 1 (control) was treated with PBS and Group 2 (treated) was treated with a reversible inhibitor of cathepsins B and L, L-264, in 100 μ l hydroxypropyl beta cyclodextrin (HPD) solution (45 % HPD, 10 % DMSO in PBS). The mice were injected (100 μ l) twice daily with saline (controls) or L-264 for 10 consecutive days at the site of the tumor. Tumors were measured with calipers and tumor volume calculated using a modified ellipsoid formula $1/2(\text{Length} \times \text{Width}^2)$. The experiment was terminated 20 days after initiation of treatment or when tumors in animals approached a volume of 1,000 mm^3 . Once the animals were sacrificed, the

different organs- kidney, liver, spleen, brain, blood and tumors were harvested for further analysis. All experiments were approved under IACUC protocol NBR-2013-004.

2.7 Small Interfering RNA Transfection for Cathepsin B Knockdown

Cathepsin B-specific small interfering RNA (siRNA) oligos were purchased from Invitrogen (Cat. Nos. 13778075, 13778-150). Stealth RNAi (or siRNA) were transfected into human SKNSH neuroblastoma cells using Lipofectamine RNAiMAX in a 24 well plate. For each well to be transfected, RNAi duplex-Lipofectamine® RNAiMAX complexes were prepared as follows.

- Add varying concentrations of RNAi duplex ranging from 10 nM to 50 nM in Opti-MEM® I Medium without serum in the well of the tissue culture plate. Mix gently.
- Mix Lipofectamine® RNAiMAX gently before use, then add 10 µl Lipofectamine® RNAiMAX to each well containing the diluted RNAi molecules. Mix gently and incubate for 10-20 minutes at room temperature.

Dilute cells in complete growth medium without antibiotics so that 500 µl contains the appropriate number of cells to give 30-50% confluence 24 hours after plating. Use 20,000-50,000 cells/well for suspension cells. To each well with RNAi duplex - Lipofectamine® RNAiMAX complexes, add 500 µl of the diluted cells. This gives a final RNA concentration ranging from 10 nM to 50 nM. Mix gently by rocking the plate back and forth. Incubate the cells for 72 hours at 37°C in a CO₂ incubator until ready to assay for gene knockdown.

Chapter 3

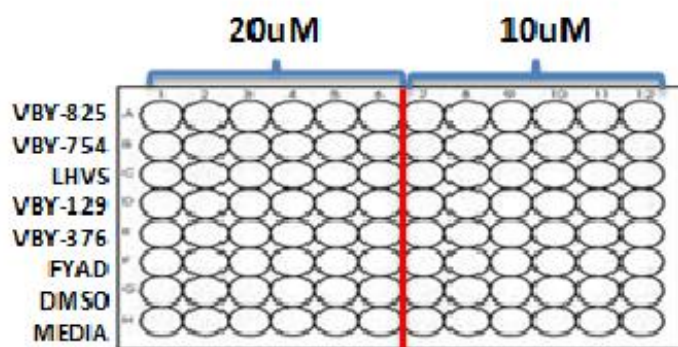
RESULTS

We have previously demonstrated that FYAD, a cathepsin B and L inhibitor, induces cell cycle arrest and apoptosis of the neuroblastoma cell lines SK-N-SH and IMR-32 in a dose dependent manner (Colella et al. 2010). Induction of apoptosis was specific to neuroblastoma cell lines, and not observed in other cancer cells and non-malignant fibroblastic cell lines (Colella et al. 2010). Apoptosis and cell cycle arrest was accompanied by accumulation of dense autophagic vesicles within inhibitor treated cells (Colella et al. 2010). In this study we investigated the effects of various inhibitors on neuroblastoma cell lines by measuring induction of cell death and inhibition of lysosomal function.

3.1 Analysis of Enzyme Activity After Addition of Inhibitors to Neuroblastoma Cells

The effect of reversible and non-reversible inhibitors of cathepsin B were tested on SKNSH neuroblastoma cells. The cells were treated with two different concentrations (20 μ M and 10 μ M) of inhibitors. The cells were seeded in a 96-well plate and each row was subjected to treatment with different inhibitors. The inhibitors used were two irreversible inhibitors of cathepsin B and cathepsin L (LHVS, FYAD), and five reversible inhibitors (L264 – an inhibitor of cathepsins B and L; VBY-825 inhibitor of cathepsin B, cathepsin L and cathepsin S, VBY-754 inhibitor of cathepsin B, cathepsin L and cathepsin S; VBY129 - a specific inhibitor of cathepsin S; and VBY376 – a specific inhibitor of cathepsin B). The cells treated with the above

inhibitors were incubated for 3 days and remaining enzyme activity was measured. For comparative analysis, we defined enzyme activity in the control as 100%. No enzyme activity remained in cells treated with either concentration of the irreversible inhibitors (Figure 3.2). The reversible inhibitor of cathepsin S (VBY-129) had no significant effect on activity against Z-Phe-Arg-NMec whereas the reversible inhibitor of cathepsin B (VBY-376) inhibited the activity by approximately 50% (Figure 3.4). However in cells treated with reversible inhibitors known to block activity of cathepsin B, L and S (VBY-825 and VBY- 754), 70 – 90% of enzyme activity was blocked (Figure 3.3). The quantification of the enzyme activity data are shown (Figure 3.5).



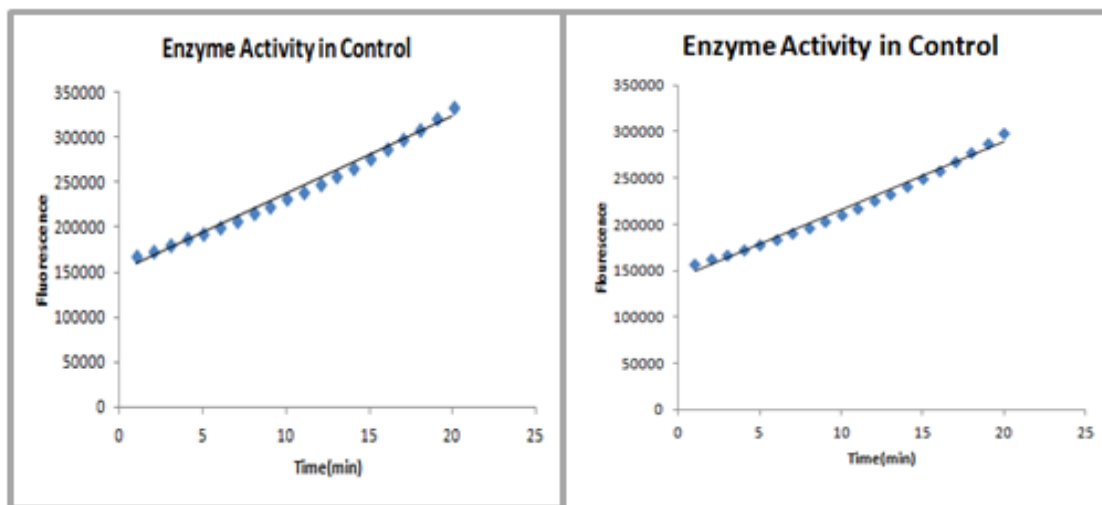
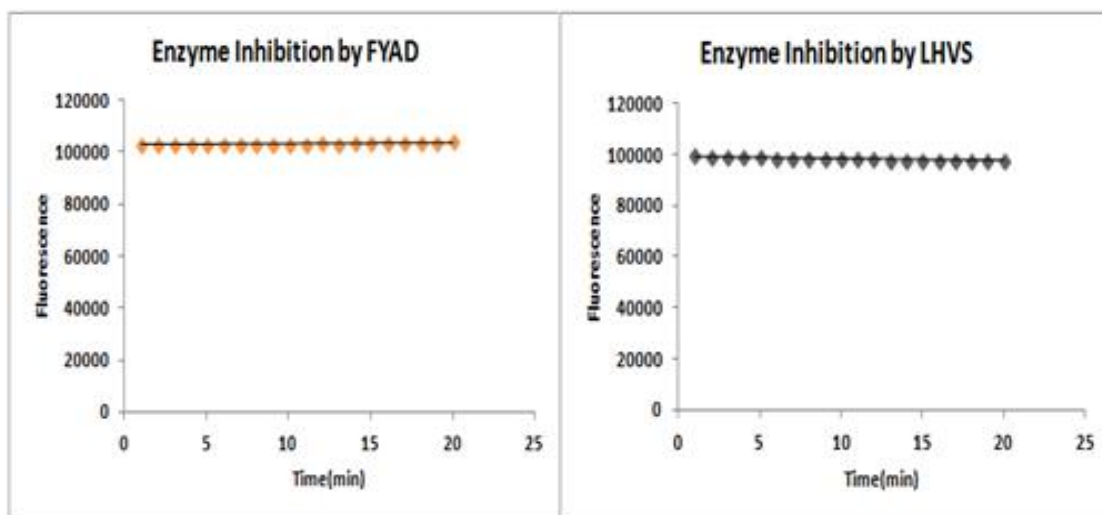


Figure 3.1: In the above figure, SKNSH cells were not treated with inhibitors and were used as control to detect the cathepsin B + L enzyme activity.

A



B

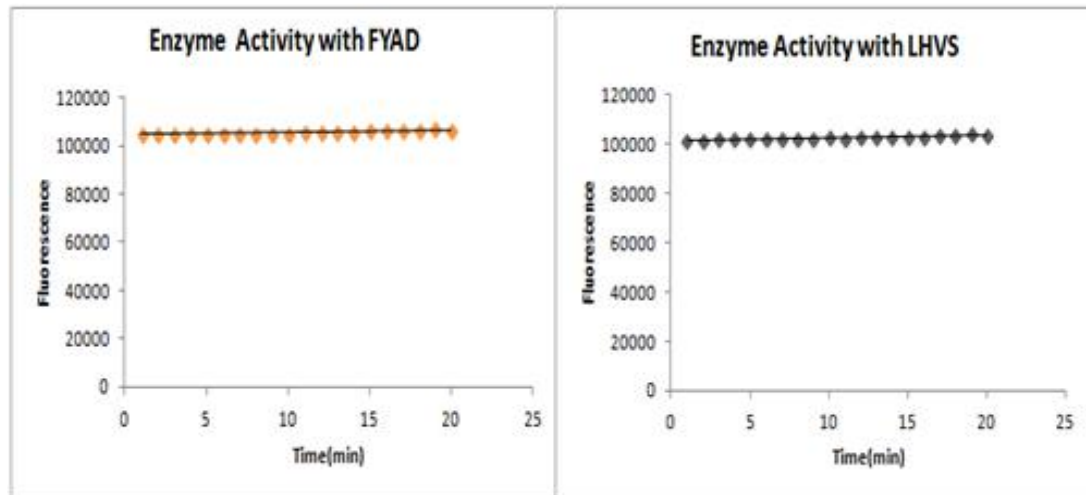
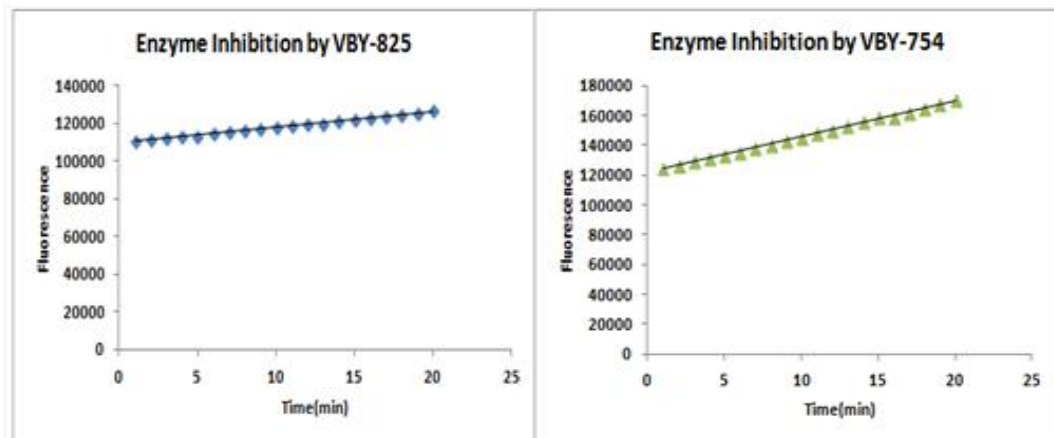


Figure 3.2: Enzyme activity of cathepsin B when treated with irreversible inhibitors FYAD and LHVS.

A, Representative images of enzyme activity assay when SKNSH cells treated with 20 μ M concentration of irreversible inhibitors FYAD and LHVS respectively. B, Representative images of enzyme activity assay when cells treated with treated with 10 μ M concentration of irreversible inhibitors FYAD and LHVS respectively.

A



B

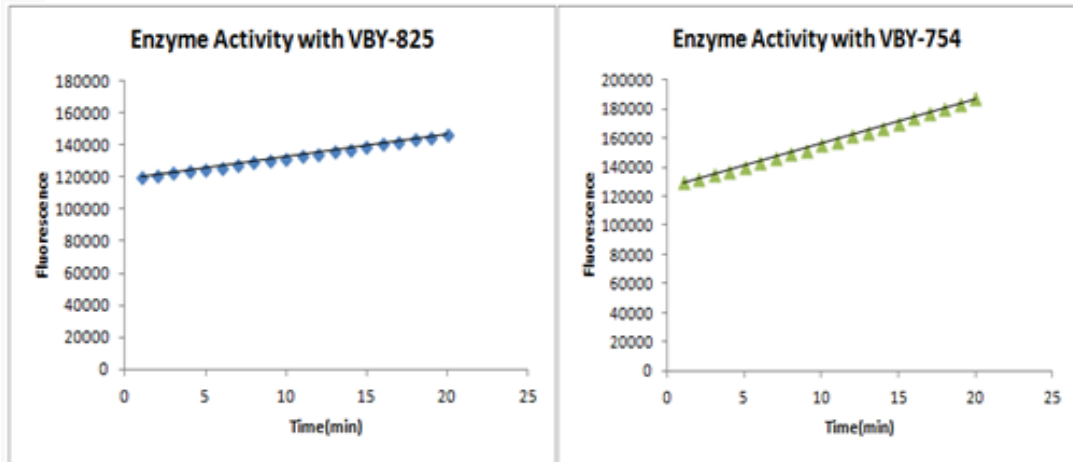
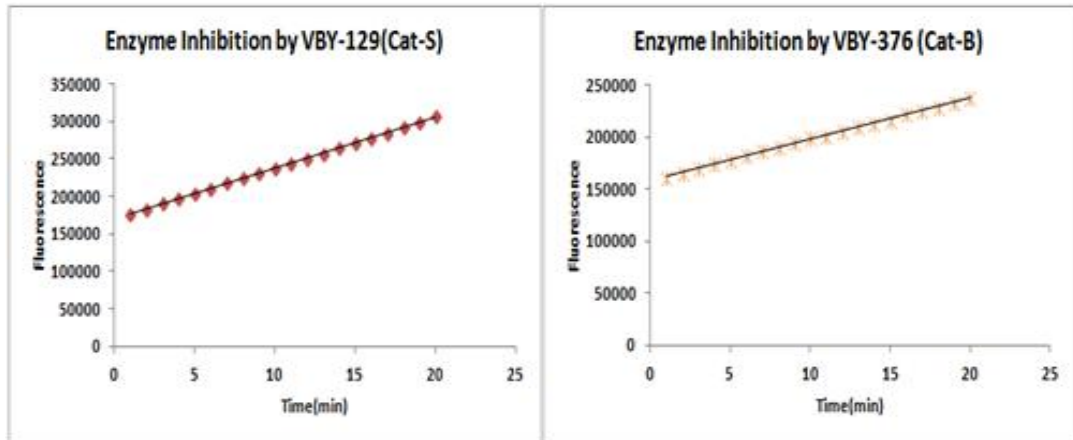


Figure 3.3: Enzyme activity of cathepsin B when treated with reversible inhibitors VB-825 (cathepsin B, L and S inhibitor) and VB-754 (cathepsin B, L and S inhibitor).

A, Representative images of enzyme activity assay when SKNSH cells treated with 20 μ M concentration of reversible inhibitors VB-825 and VB-754 respectively. B, Representative images of enzyme activity assay when SKNSH cells treated with 10 μ M concentration of reversible inhibitors VB-825 and VB-754 respectively.

A



B

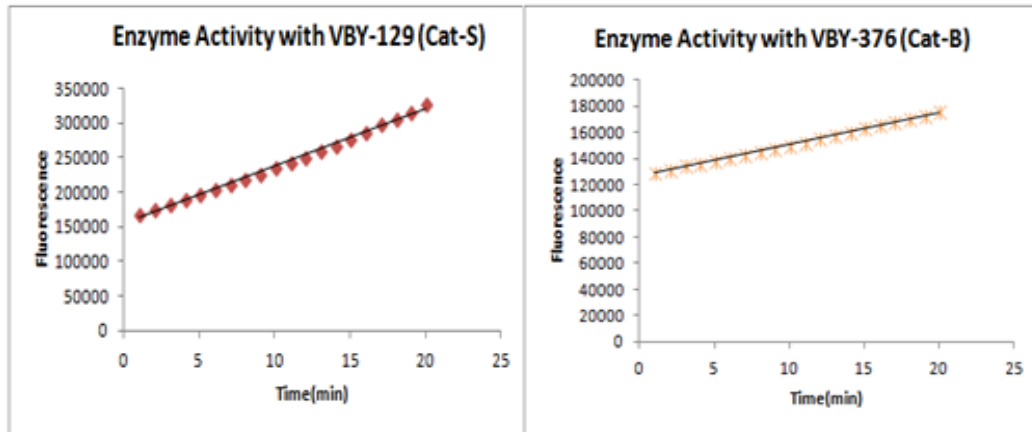


Figure 3.4: Enzyme activity of cathepsin B when treated with reversible inhibitors VB-129 (cathepsin S inhibitor) and VB-376 (cathepsin B inhibitor).

A, Representative images of enzyme activity assay when SKNSH cells treated with 20 μ M concentration of reversible inhibitors VB-129 and VB-376 respectively.

B, Representative images of enzyme activity assay when SKNSH cells treated with 10 μ M concentration of reversible inhibitors VB-129 and VB-376 respectively.

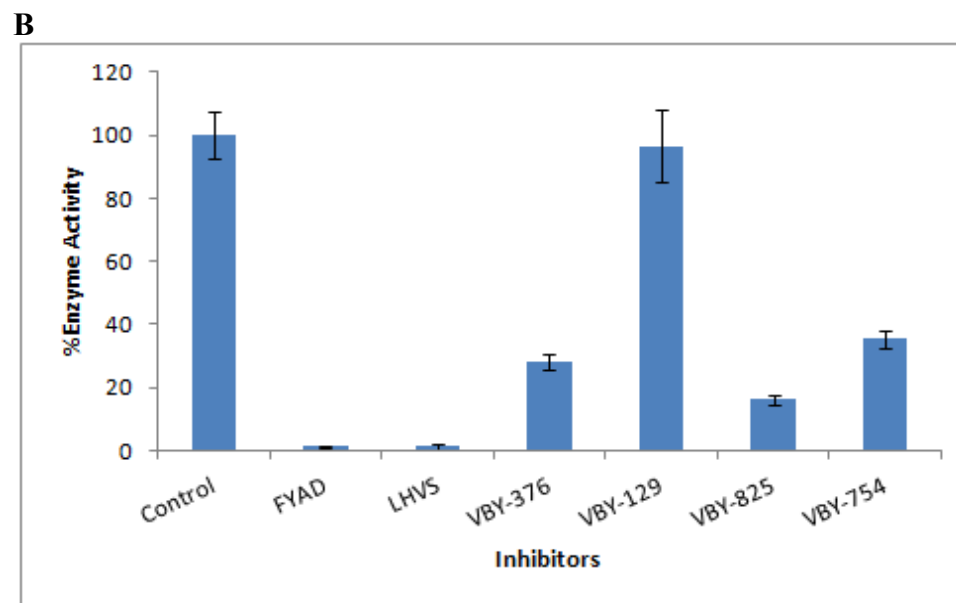
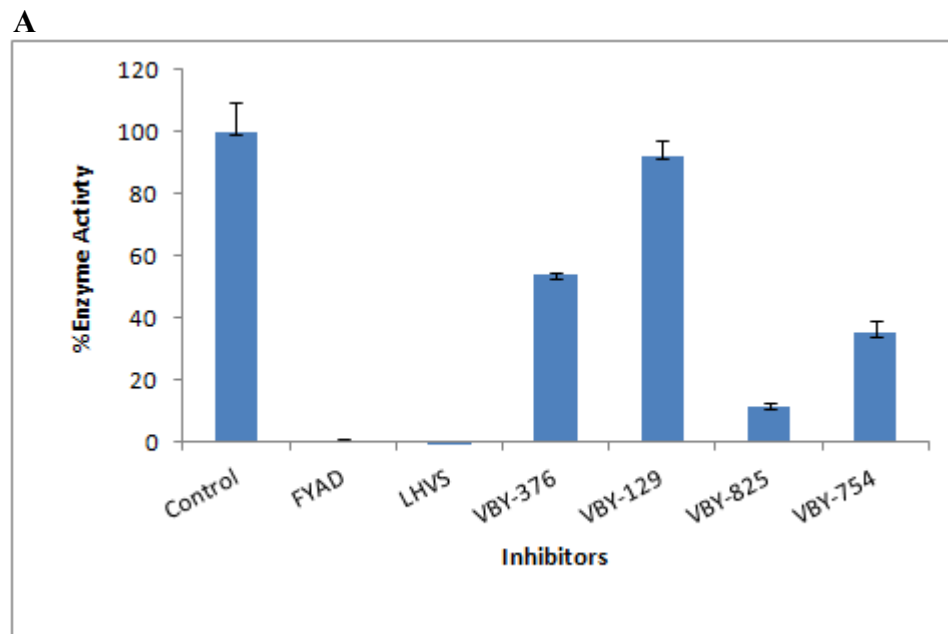


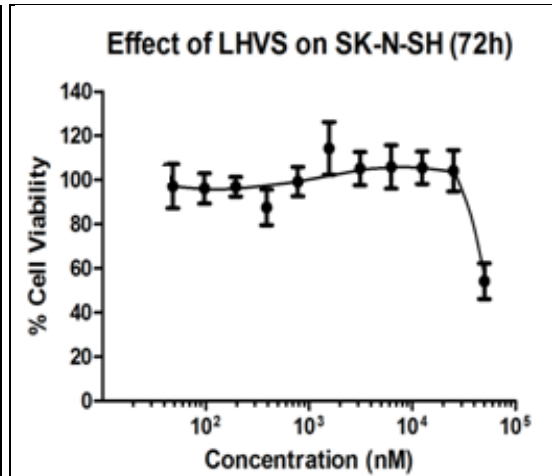
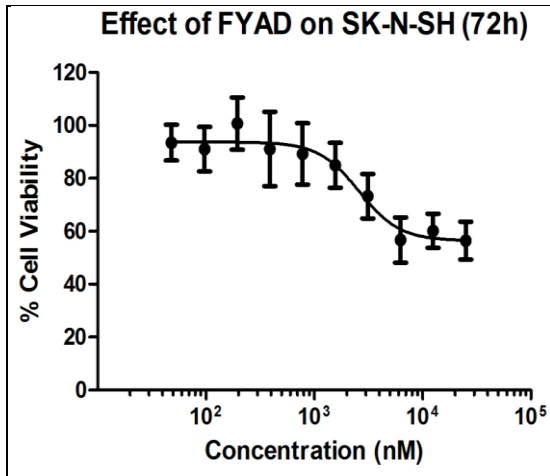
Figure 3.5: Comparative representation of enzyme activity of cathepsins B and L when treated with various reversible and irreversible inhibitors on SKNSH cells.

A, Representation of the various enzyme activities of cathepsin B when SKNSH cells are treated with 20 μ M concentration of the different inhibitors. B, Representation of the various enzyme activities of cathepsin B when SKNSH cells are treated with 10 μ M concentration of the different inhibitors. Values are mean of six measurements and bars show standard deviation.

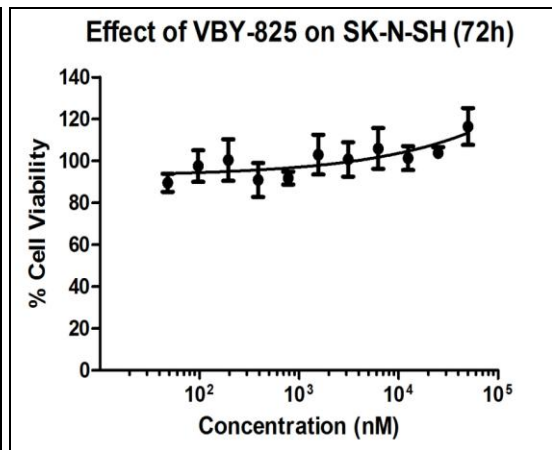
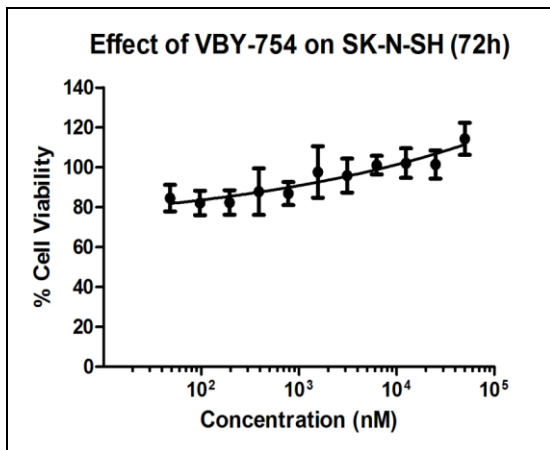
3.2 Dose-Dependent Effect of Inhibitors on Neuroblastoma Cell Viability

SK-N-SH cells were treated either with the vehicle (control) or protease inhibitors for 72 h as described in materials and methods. The cells were treated with a series of concentration of reversible or irreversible inhibitors of cathepsins B and L and our results show that there was a decrease in cell viability in the cells that were treated with the irreversible inhibitor FYAD, as shown previously. LHVS only caused a reduction in cell viability at the highest concentration. The reversible inhibitors that blocked the activity of cathepsin B, L and S (VBY-754, VBY-825) did not impact cell viability at any concentration. A decrease in cell viability was seen in cells treated with high levels of a cathepsin S specific inhibitor (VBY129) and cathepsin B specific inhibitor (VBY-376) but it was noted that these compounds precipitated at the higher concentrations and consequently cell viability was impacted by non-specific solubility issues.

A



B



C

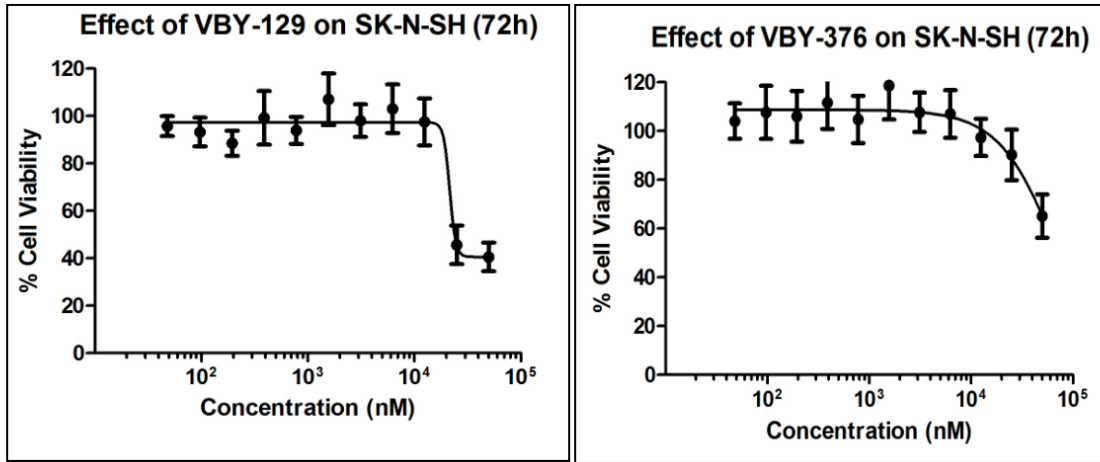


Figure 3.6: Concentration effect of cathepsin inhibitors on neuroblastoma cell survival.

A-C shows SK-NSH cells were treated with FYAD, LHSV, VBY-825, VBY-754, VBY-129, VBY-376 (4.5×10^2 nM - 5×10^5 nM), or with DMSO vehicle control. Media supplemented with individual inhibitors or with vehicle control was added to the cells and incubated for three days. At the end of incubation, viability was measured using cell titer blue.

3.3 Accumulation of Cleaved LC-3 in Inhibitor Treated Neuroblastoma Cells.

Accumulation of processed LC-3, a known marker of autophagy, indicates significant induction of autophagy. Previous studies have shown that in untreated conditions the primary form of LC-3 corresponds to the uncleaved form that is cytosolic, whereas in treated cells there is a major portion of the cleaved form that is incorporated into membranes of autophagic vesicles. Western blot analysis revealed the accumulation of a cleaved form of LC-3 (LC3-II) in cells treated with the

irreversible inhibitors FYAD and LHVS (Figure 3.7). LC3-II bands were also seen when treated with the two reversible inhibitors of both cathepsins B and L, VBY-754 and VBY-825. This was not the case with the VBY-129 cathepsins S inhibitor and LC-3 was only partially processed in cells treated with the VBY-376 cathepsin B inhibitor.

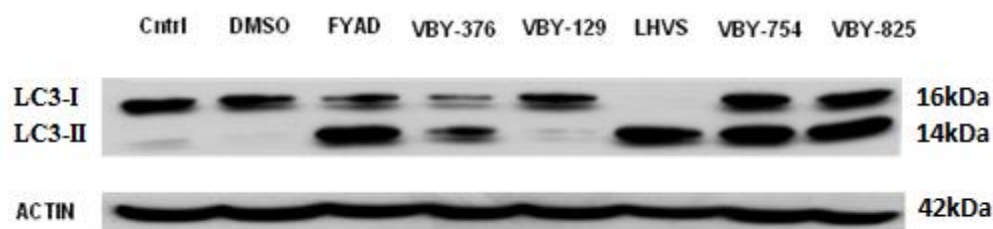


Figure 3.7: Accumulation of LC-3 in inhibitor treated neuroblastoma cells.

SK-N-SH cells were treated with protease inhibitors as described in materials and methods, then whole cell lysates were harvested and subject to immunoblotting. The cleaved form of LC-3 was seen at very low levels in untreated condition, but in irreversible inhibitor treated cells it showed a dramatic increase.

3.4 Cathepsin B Knockdown by Small Interfering RNA(siRNA) Transfection

Silencer® Select Validated siRNAs are individual siRNA duplexes that have been verified experimentally to reduce the expression of their individual target genes. Each siRNA has been functionally confirmed and is guaranteed to reduce target gene expression by at least 80% when measured 48 hours post- transfection.. Varying concentrations of control siRNA sequences and cathepsin B siRNA sequences were transfected respectively ranging from 10 nM to 50 nM. The efficacy of the knockdown

of cathepsin B was shown by the significant decrease in the cathepsin B levels when compared to the controls at all concentrations of siRNA used (Figure 3.8).

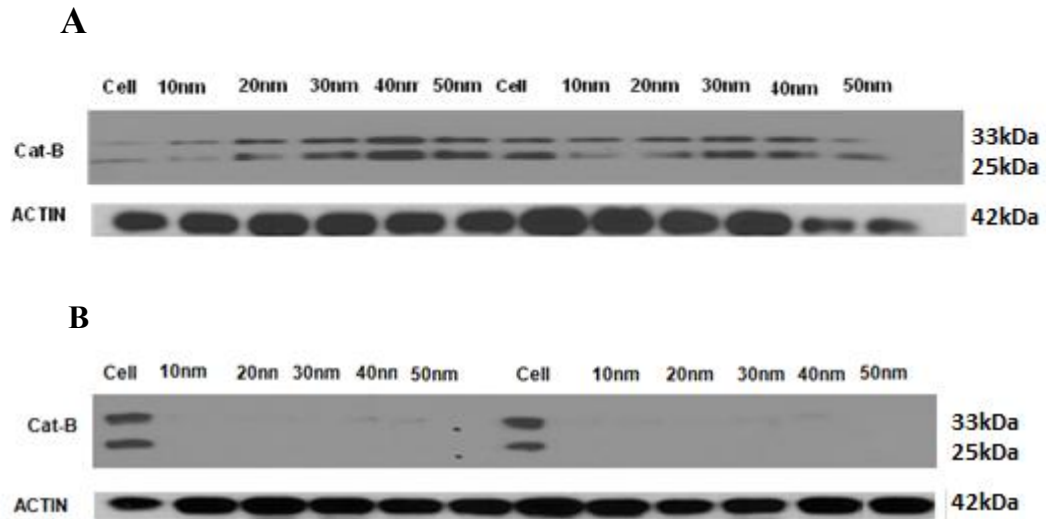


Figure 3.8: Cathepsin B knockdown by small interfering RNA(siRNA) Transfection. SKNSH cells were treated with varying concentrations of control and cathepsin B siRNA respectively ranging from 10 nM to 50 nM. A, SKNSH cells were transfected with control siRNA for 72 hrs and western blot analysis shows cathepsin B protein levels at different siRNA concentrations thereby revealing no significant knockdown of the protein levels. B, SKNSH cells were transfected with cathepsin B siRNA for 72hrs and western blot analysis shows cathepsin B protein levels at different siRNA concentrations. It signifies the effecting knockdown of cathepsin B protein levels when compared to the controls

3.5 Cathepsin B and L Knockdown by Combining Small Interfering RNA(siRNA) Transfection and Cathepsin B and L Inhibitor FYAD

In this trial, we combined cathepsin B and L siRNA transfection along with irreversible inhibitor (FYAD) to determine if sensitivity of the cells towards the inhibitor increased. Our results showed that siRNA knock down of both cathepsins B and L did not affect cell viability directly and did not enhance sensitivity to FYAD. We were not able to show effectiveness of siRNA of down-regulation of cathepsin L because the antibody against this enzyme was not sufficiently sensitive to detect the protein in these cells. Knockdown of cathepsin B was approximately 80%. We have previously shown that more than 90% of the activity against cathepsins B and L needs to be blocked to cause death in these cells and consequently were unable to demonstrate the critical role of cathepsins B and L in neuroblastoma cell survival using siRNA technology.

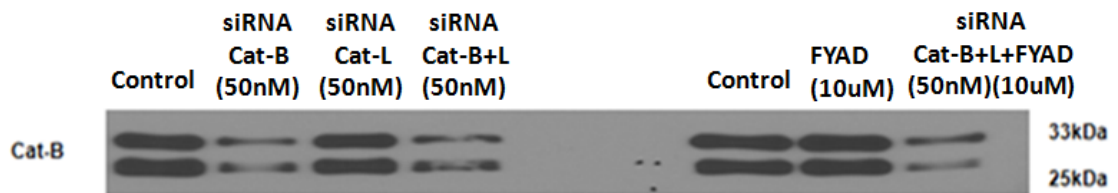


Figure 3.9: Cathepsin B knockdown by combining small interfering RNA(siRNA) Transfection and cathepsin inhibitor FYAD.

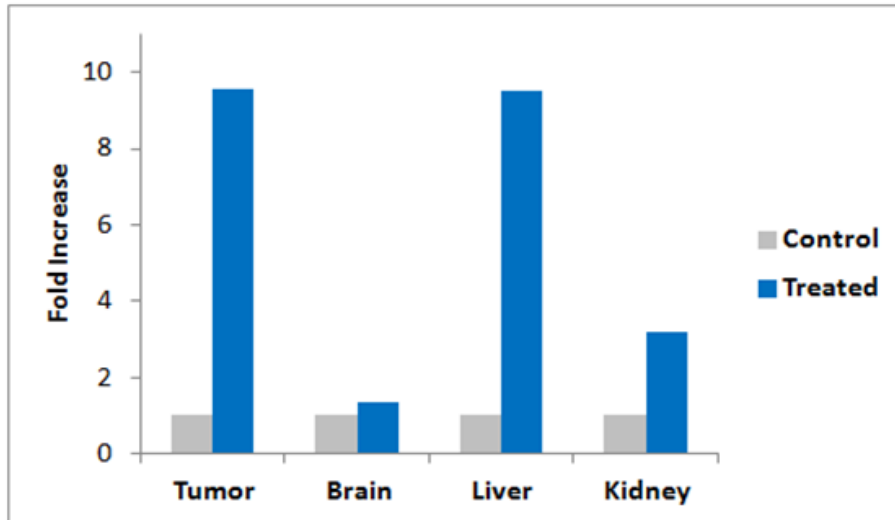
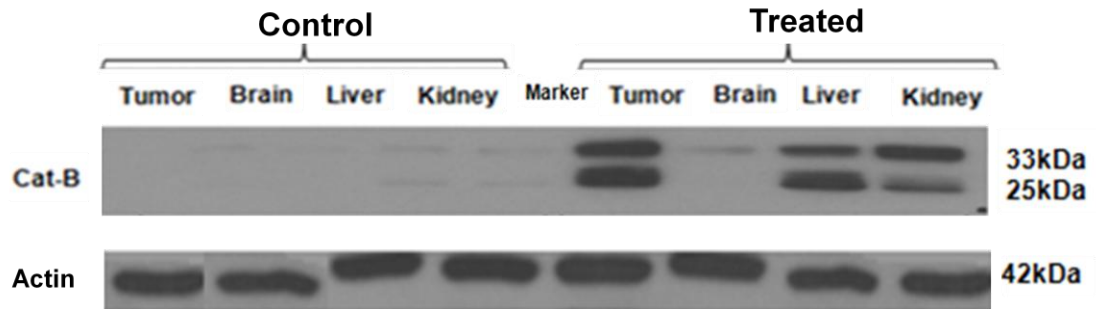
SKNSH cells were treated with 50 nM concentration of cathepsin B siRNA, cathepsin L siRNA and cathepsin B and L siRNA respectively. SKNSH cells were also treated with 10 μ M FYAD and cathepsin B,L siRNA and FYAD in combination respectively. SKNSH cells were transfected with various combination of siRNA and inhibitor for

72 h and western blot analysis shows that there was no significant changes when used in cathepsin B, L siRNA and FYAD in combination.

3.6 *In vivo* Characterization of the Effects of L264, Reversible Cathepsin B Inhibitor

Treatment of sub-cutaneous tumors with L-264 twice daily for 10 days failed to arrest tumor growth (data not shown). During time of injections, measurement of tumor volume by calipers was complicated due to the effect of the volume of drug and vehicle control injected at the tumor site. Significant differences in volume were not detected between control and treated animals. However, after cessation of treatment, tumor volumes were significantly higher in treated animals than controls at all time-points (data not shown). In separate experiments, tissues from treated and control animals were excised after completion of dosage with inhibitor. After the 10 day treatment of L264, the control and the treated animals were euthanized and organs were harvested to determine the effect of treatment on cathepsin B protein levels. Kidney(3-15 fold increase), liver(9-18 fold increase) and tumor (10-90 fold increase) samples showed a significant increase in the cathepsin B protein levels in the treated animals when compared to that of the controls. However, cathepsin B levels in the brain of the treated animals did not show any increase in the protein levels which illustrates that the drug is not effective against proteases in brain.

A



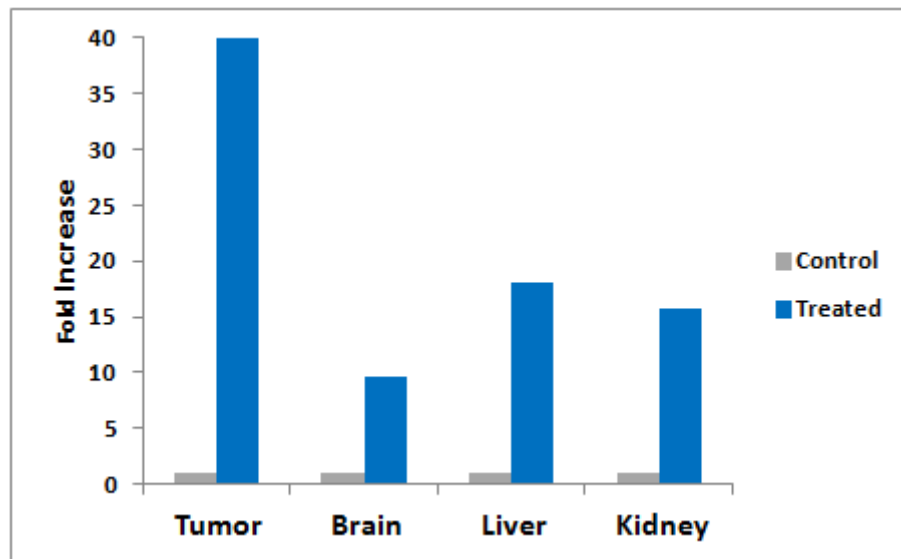
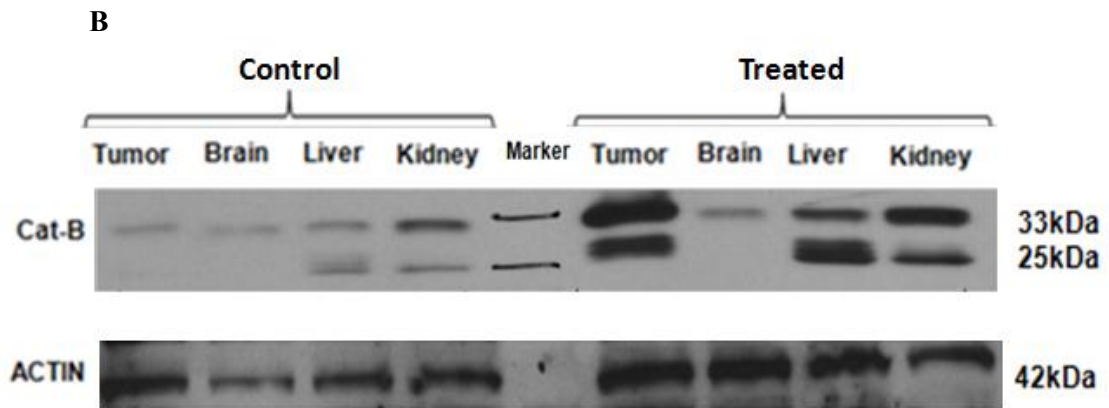


Figure 3.10: *In vivo* characterization of the effects of L264, reversible cathepsin B inhibitor.

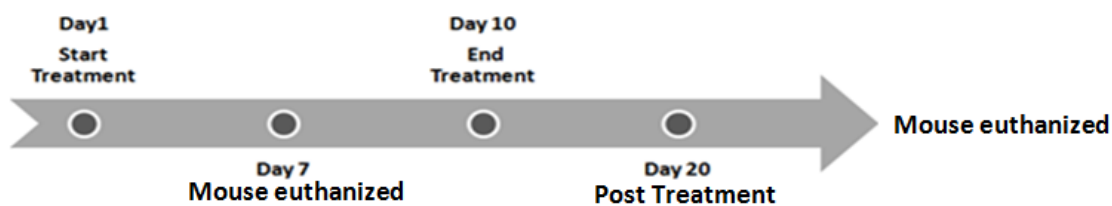
10^7 SK-N-SH cells were injected subcutaneously into two groups of 10 hairless/SCID mice. When the first tumors were visible, vehicle or L264 was injected at the tumor site and tumors measured daily with calipers. After treatment the animals were excised and tissue samples were collected from vehicles and treated animals. A and B show

two separate sets of tissue samples from treated and control animals. Western blots of control and treated samples were exposed to film in the same cassette to ensure identical exposure to enable comparative analysis. Fold increase of cathepsin B relative to control animals from untreated animals is shown below. A dramatic increase in levels of cathepsin B protein in kidney, liver and tumor were seen, compared to the control samples.

3.7 Levels of Cathepsin B Protein in Tumors During and After Treatment with L264

In this part of the study we wanted to examine the effects of the drug L264 on cathepsin B protein levels in the tissues post treatment. SKNSH cells injected into hairless/SCID mice, divided equally into vehicles and treated. Among the treated group equal number of mice were sacrificed at different time points during treatment and the others continued all ten days of treatment and were sacrificed after they were placed under observation for ten days post treatment. Tissue samples were collected from all the sample and cathepsin B protein levels were estimated by Western Blot analysis.

A



B

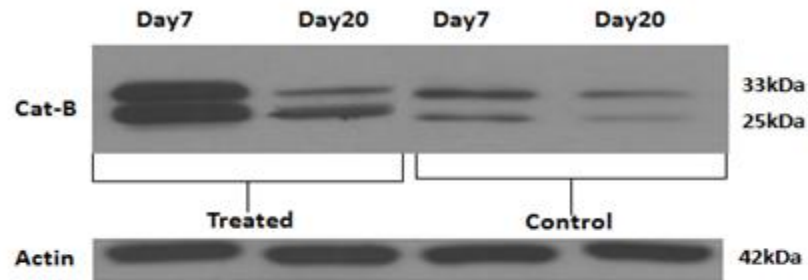


Figure 3.11: Cathepsin B protein levels in tumors during and after treatment with L264.

10^7 SK-N-SH cells were injected subcutaneously into two groups of hairless/SCID mice. When the first tumors were visible, vehicle or L264 was injected at the tumor site and tumors measured daily with calipers. One group of treated and control animals were sacrificed on day 7. A second group continued treatment for ten days and were placed under observation for ten more days. These animals were sacrificed ten days post treatment. Tissue samples were collected from vehicles and treated animals. A, Representation of the time frame of the experiment depicting the various time points at which the animals were sacrificed. B, Western blotting was used to show levels of cathepsin B in tumor tissue. 10 days after ending of treatment, levels of cathepsin B in tumors of treated animals returned to levels in tumors of control animals.

3.8 Arrest of Tumor Growth In Vivo by K11777, Irreversible Cathepsin B Inhibitor

Treatment of subcutaneous tumors with K11777 twice daily for 10 days arrested tumor growth. During time of injections, measurement of tumor volume was done by using calipers and significant differences in volume were detected in control and treated animals. After cessation of treatment, tumor volumes were significantly lower in treated animals than controls at all time-points.

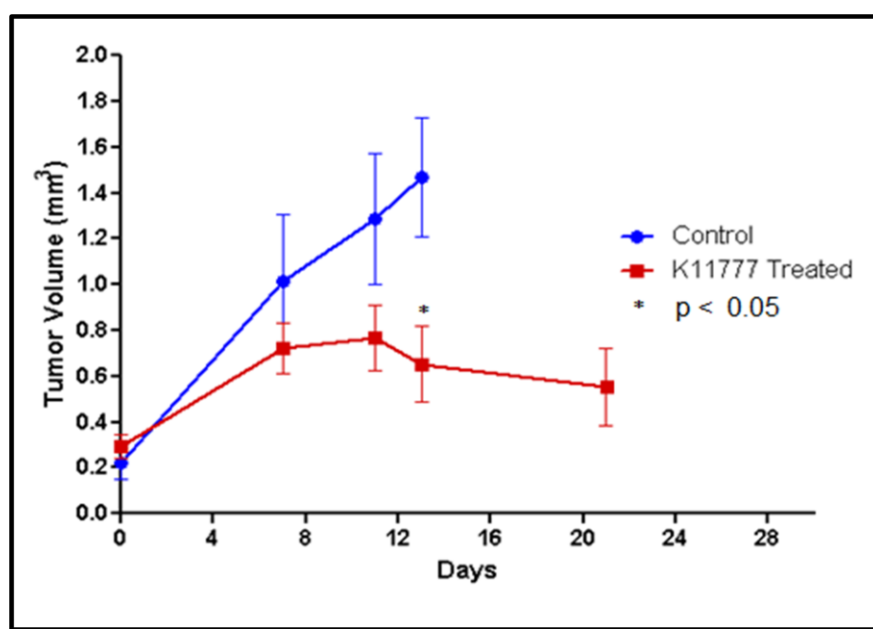
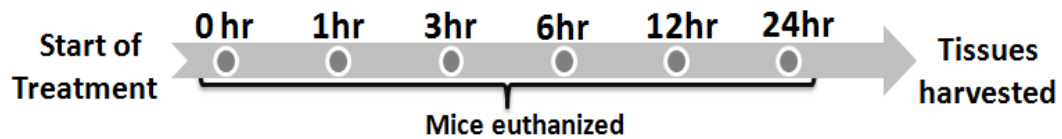


Figure 3.12: Effects of K11777 on tumor growth *in vivo*. 10^7 SK-N-SH cells were injected subcutaneously into hairless/SCID mice.

When the first tumors were visible, vehicle or K11777 was injected at the tumor site and tumors measured daily with calipers. Tumors were significantly smaller in treated animals. An asterisk denotes $p < 0.05$. Control animals did not survive beyond 13 days.

3.9 Effects on Enzyme Activity of Various Tissues due to Cathepsin Inhibition by Drug K11777

In a different set of experiments, K11777 was administered to 6 week old Scid hairless outbred mice strain code 474 (purchased from the Jackson Laboratories) and tissues harvested at 0, 1, 3, 6, 12 and 24 hours after treatment. Tissue was homogenized and enzyme activity measured. In liver and kidney tissue when the drug was injected at 0 hr, 1 hr and 3 hrs, there is a drop in the cathepsin enzyme activity. By 6 hrs there is a gradual increase in the cathepsin enzyme activity. Figure 3.13 shows that by 24 hours the cathepsin enzyme activity returns to normal. However in the brain tissue there was no significant change in the cathepsin enzyme activity over a period of 0 - 24 hours which indicates that in vivo, K11777 inhibits cathepsin activity by over 70% but is not effective against proteases in brain.



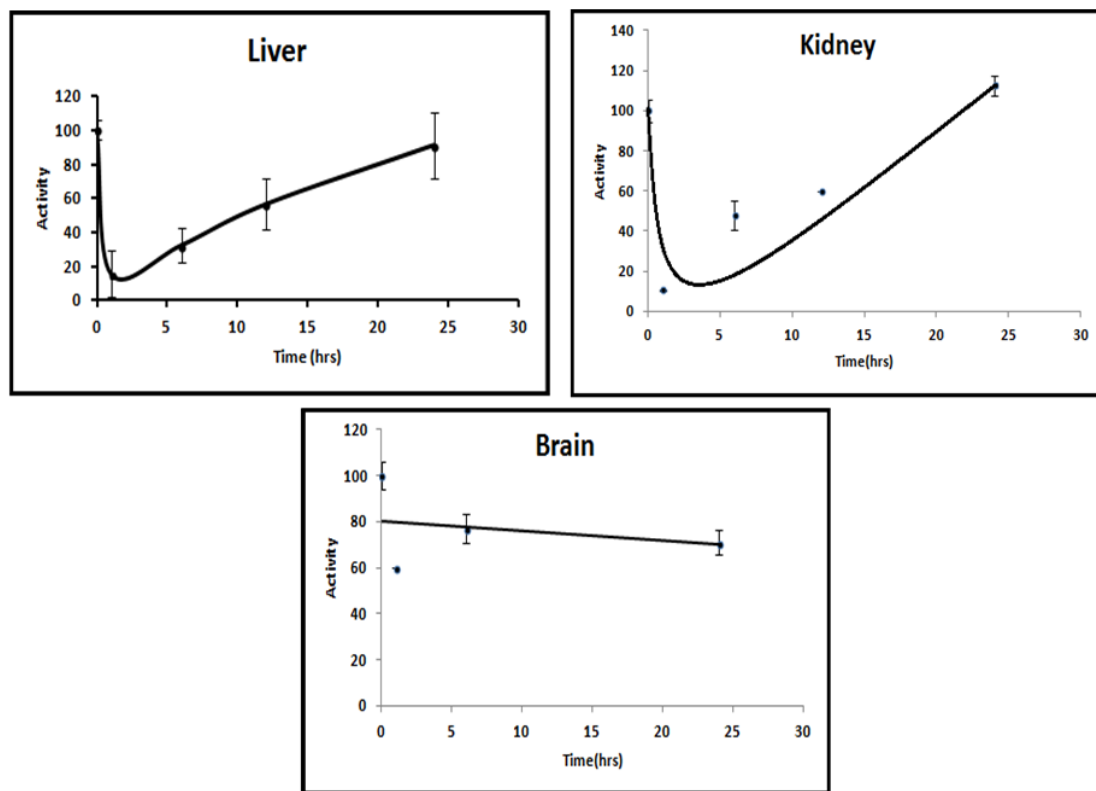


Figure 3.13: Effects of K11777 on cathepsin enzyme activity *in vivo*.

Mice were injected subcutaneously with the drug K11777 and tissue harvested at regular intervals of 0, 1, 3, 6, 12 and 24 hours. Liver, kidney and brain tissues were harvested from each animal. Cathepsin enzyme activity was measured at the given time intervals. A drop in activity levels were seen in the liver and kidney samples before returning to normal levels by 24 hours. By contrast, activity levels in brain did not significantly change over time.

Chapter 4

DISCUSSION

Although neuroblastoma is a unique pediatric cancer, current therapies were originally developed for more common adult cancers and adapted for use in children. Unfortunately the major cytotoxic chemotherapies have severe side-effects in children and the response of advanced neuroblastoma to current therapies is poor. In previous studies, it has been shown that inhibition of the lysosomal proteases cathepsins B and L induces selective apoptosis of neuroblastoma cells without affecting normal or other cancer cells lines. Induction of apoptosis was preceded by accumulation of autophagic vesicles within inhibitor treated cells, suggestive of a role for autophagy in inducing cell death. The primary goal of this study was to more rigorously test the hypothesis that inhibition of cathepsins B and L causes cell death in neuroblastoma cells using compounds that are already being developed in programs targeting similar enzymes as new therapeutic approaches to treat other ailments.

4.1 Efficacy of Compounds to Induce Neuroblastoma Cell Death Depends on the Inhibition of Cathepsin B and L Enzymes.

A diverse group of reversible and irreversible cathepsin inhibitors were evaluated for their ability to inhibiting neuroblastoma tumor cell growth. Previous studies have shown that FYAD (Fmoc-Tyr-Ala-CHN₂) binds to both cathepsins B and L and that complete inhibition of both of these enzymes is maintained in cultured neuroblastoma cells, creating a chemical knockout of both enzyme activities. It was also shown that at least 90% inhibition of cathepsins must be achieved in order to

cause SKNSH cell death. In this study, I showed that two irreversible inhibitors of cathepsins B and L, FYAD and LHVS, efficiently inhibited enzyme activity at the two different concentrations (Fig 3.2) used. The added inhibitor concentration of 10 – 20 μM may be lower than the concentration of enzymes in lysosomes, which can be in the millimolar range, so mechanisms for increasing compound concentration in lysosomes are required to ensure effectiveness of reversible inhibitors. Once inhibitor diffuses into the lysosome it will bind to enzyme and maintain a concentration gradient of free inhibitor until all enzyme is inhibitor bound. Thus even very low concentrations of inhibitors should eventually block activity of cathepsins B and L. Steady-state levels of activity will depend upon the rate at which enzymes are inactivated and rate of synthesis of new enzyme.

The kinetics for inhibition by reversible inhibitors will be different. VBY-825 is a reversible cathepsin B, L and S inhibitor which that showed only 80% enzyme inhibition. VBY-754 is a reversible inhibitor with a similar enzyme target specificity that only showed an enzyme inhibition of approximately 60%. These two inhibitor were not effective in impairing growth of SKNSH cells. VBY-376, a specific reversible inhibitor of cathepsin B, blocked enzyme activity by 80% and VBY 129, a specific reversible inhibitor of cathepsin S, did not block enzyme activity in cells. Although high concentrations of these two inhibitors appeared to induce cell death (Fig 3.6) the drugs were clearly insoluble and the precipitates may have had an indirect effect on cell survival.

For reversible inhibitors, the kinetics of inhibition of high concentrations of enzymes in lysosomes is very complex. In standard Michaelis-Menten kinetics enzymes are efficiently inhibited if inhibitor concentration is much higher than K_i for

enzyme inhibition. However this assumes low enzyme concentration and negligible reduction in free inhibitor concentration. Thus in the lysosome inhibition will be inefficient and although binding of inhibitor to the enzyme will create a concentration gradient that favors further influx of inhibitor, this is not likely to lead to efficient enzyme inhibition.

We also tried to generate siRNA techniques to knock down expressions of cathepsin B and/or L (Fig 3.8). Unfortunately we were not able to knock down expression of cathepsin B by more than 80% which we know from prior inhibitor studies to be insufficient to cause cell death of SK-N-SH cells (Colella et al 2010). We also combined siRNA transfection and with inhibitor treatment (Fig 3.9) but were unable to demonstrate any increased sensitivity of neuroblastoma cells to inhibitor treatment. Cathepsin B is expressed at very high levels in most cell types, so complete knockdown of enzyme by RNAi is particularly difficult and consequently we were unable cause neuroblastoma cell death use RNAi technology.

4.2 Autophagy is Related to the Cell Death Caused by the Treatment of the Inhibitors

Neuroblastoma cell death caused by cathepsin inhibition may be due to the accumulation of proteins that are normally degraded by cathepsin B and L. Previous studies have shown that cell death was preceded by the induction of markers of cell stress and autophagy. Efficacy of each inhibitor of cathepsins B and L in causing cell death corresponded with appearance of LC3-II, the lipidated form of LC-3, a key step in the formation of autophagosomes. Figure 3.7 shows that that is an increased level of LC3-II bands seen in the two irreversible inhibitors FYAD and LHVS when compared to the controls and the reversible inhibitors VBY 129 and VBY 376. This supports

prior conclusions that the induction of cell death in the cells treated with the irreversible inhibitors is due to the accumulation of un-degraded proteins leads to the induction of apoptosis that is preceded by accumulation of autophagic vesicles.

4.3 Effects of Reversible Inhibitor L264 on Neuroblastoma Cell Growth In Vivo

Previous studies have shown that 100 nM of reversible inhibitor L264 was required to induce 90% enzyme inhibition and higher concentrations were required to cause neuroblastoma cell death in vitro. The effectiveness of enzyme inhibition in vivo by reversible inhibitors is more difficult to determine. L264 failed to arrest growth of neuroblastoma tumors in a xenograft mouse model. L264 dramatically increased levels of cathepsin B protein in mouse liver, kidney and tumor (Fig 3.10). It did not affect levels of cathepsin B in the brain, indicating that the compound did not cross the blood brain barrier or enter the central nervous system. Although cathepsin levels were elevated during treatment, they returned to normal levels 10 days after treatment (Figure 3.11). Increased steady state levels of cathepsin B could be caused by reduced turnover of cathepsin B by itself or other cathepsins. This would not be a problem for irreversible inhibitors that remain bound to enzyme and continue to prevent activity on removal of free inhibitor by either inactivation or loss into urine. Reversible inhibitors do not form any covalent bonds with the enzyme and hence when free inhibitor is removed from the system the enzyme and inhibitor complex can dissociate and enzyme activity restored. Thus if free inhibitor is not maintained at a high level, enzyme inhibition will not be maintained and as it has been shown that levels of enzyme increase in inhibitor treated animal tissues and tumor, reversible inhibitor treatment may actually increase enzymatic activity in tumors. This may in part

explain why L264 was not effective as a treatment for neuroblastoma in our model system.

4.4 Cathepsin Inhibition by Irreversible Inhibitor K11777 Reduces Neuroblastoma Cell Growth

In contrast to L-264, K11777 was shown to inhibit growth of neuroblastoma tumors in a xenograft mouse model (Fig 3.12). K11777 inhibited activity of cathepsins B and L in mouse liver and kidney but does not appear to readily cross the blood brain barrier to inhibit cathepsins in the central nervous system.

Although tumor growth was impaired, the treatment protocol did not result in eradication of tumors. Cathepsin activity was inhibited by approximately 70 % in vivo but our in vitro studies indicated that more than 90 % inhibition is required to induce cell death. However, a level of inhibition sufficient to reduce cell growth was achieved. Thus the primary effect of K11777 (Fig 3.13) in vivo appears to be slow tumor growth by inhibition of cathepsin enzyme activity. Cathepsin inhibition restricts growth of many cancer cell types both in vitro and in vivo and may be caused by effects on cell proliferation, tumor cell invasion or angiogenesis.

4.5 Inhibitors for Cathepsins B and L for Potential Clinical Use

The panel of inhibitors used in this study was chosen because their bioavailability and efficacy have already been demonstrated in other clinical and preclinical programs that target similar proteases. The reversible nitrile inhibitors have been developed in a program to target cathepsin K to treat osteoporosis. Halting the progression of osteoporosis does not require complete inhibition of cathepsin K so reversible inhibitors may be appropriate for treating this disease. Our studies indicate that the reversible inhibitors are not good candidates for treating neuroblastoma

because even if treatment regimens could be designed to maintain high concentrations of active compounds in the target tissues, an increased level of total cathepsin protein would require even more efficient enzyme inhibition. A related inhibitor that is more specific for cathepsin K is currently in phase 3 clinical trials to treat osteoporosis. (Castrillon JL et al 2010).

K11777, an irreversible peptidyl vinyl sulfone inhibitor, is being developed to target cathepsin-like proteases of *Trypanosoma cruzi* as a novel treatment for Chagas disease. The effect of K11777 on neuroblastoma cells both in vivo and in vitro provides proof of concept that irreversible inhibition of cathepsins B and L offers a potential novel therapeutic approach to treat neuroblastoma. This result mirrors our prior study showing that the laboratory reagent FYAD also impaired tumor cell growth in vivo (Colella et al 2010). A limitation of these compounds is that we have not been able to completely inhibit cathepsin activity in our animal model system. Also, in our study we limited treatment to 10 days to reduce treatment time to diminish non-specific effects of intratumor injections. K11777 is orally bio-available and could also be delivered i.p. for more long-term treatment protocols. Unlike standard chemotherapeutic approaches, these cathepsin inhibitors show remarkably low toxicity in pre-clinical animal studies and clinical trials. Adoption of compounds from therapeutic studies that are already in clinical trials may accelerate the development of a new treatment for neuroblastoma.

REFERENCES

(Neuroblastoma)

Alva, A. S., S. H. Gultekin, et al. (2004). "Autophagy in human tumors: cell survival or death?" *Cell Death Differ* 11(9): 1046-8.

Amaravadi, R. K., D. Yu, et al. (2007). "Autophagy inhibition enhances therapy-induced apoptosis in a Myc-induced model of lymphoma." *J Clin Invest* 117(2): 326-36.

Ambroso, J. L. and C. Harris (1994). "In vitro embryotoxicity of the cysteine proteinase inhibitors benzyloxycarbonyl-phenylalanine-alanine-diazomethane (Z-Phe-Ala-CHN₂) and benzyloxycarbonyl-phenylalanine-phenylalanine-diazomethane (Z-Phe-Phe-CHN₂)." *Teratology* 50(3): 214-28.

Barrett, A. J. and H. Kirschke (1981). "Cathepsin B, Cathepsin H, and cathepsin L." *Methods Enzymol* 80 Pt C: 535-61.

Brodeur, G. M., J. Pritchard, et al. (1993). "Revisions of the international criteria for neuroblastoma diagnosis, staging, and response to treatment." *J Clin Oncol* 11(8): 1466-77.

Brodeur, G. M., R. C. Seeger, et al. (1988). "International criteria for diagnosis, staging, and response to treatment in patients with neuroblastoma." *J Clin Oncol* 6(12): 1874-81.

Cartledge, D. M., R. Colella, et al. (2012). "Inhibitors of cathepsins B and L induce autophagy and cell death in neuroblastoma cells." *Invest New Drugs* 31(1): 20-9.

Castino, R., D. Pace, et al. (2002). "Lysosomal proteases as potential targets for the induction of apoptotic cell death in human neuroblastomas." *Int J Cancer* 97(6): 775-9.

Castleberry, R. P., J. J. Shuster, et al. (1994). "The Pediatric Oncology Group experience with the international staging system criteria for neuroblastoma. Member Institutions of the Pediatric Oncology Group." *J Clin Oncol* 12(11): 2378-81.

- Chang, C. P., M. C. Yang, et al. (2007). "Concanavalin A induces autophagy in hepatoma cells and has a therapeutic effect in a murine in situ hepatoma model." *Hepatology* 45(2): 286-96.
- Chwieralski, C. E., T. Welte, et al. (2006). "Cathepsin-regulated apoptosis." *Apoptosis* 11(2): 143-9.
- Clancy, B., R. B. Darlington, et al. (2001). "Translating developmental time across mammalian species." *Neuroscience* 105(1): 7-17.
- Colella, R., G. Lu, et al. (2010). "Induction of cell death in neuroblastoma by inhibition of cathepsins B and L." *Cancer Lett* 294(2): 195-203.
- Crawford, C., R. W. Mason, et al. (1988). "The design of peptidyl-diazomethane inhibitors to distinguish between the cysteine proteinases calpain II, cathepsin L and cathepsin B." *Biochem J* 253(3): 751-8.
- Dauth, S., R. F. Sirbulescu, et al. (2011). "Cathepsin K deficiency in mice induces structural and metabolic changes in the central nervous system that are associated with learning and memory deficits." *BMC Neurosci* 12: 74.
- Degenhardt, K., R. Mathew, et al. (2006). "Autophagy promotes tumor cell survival and restricts necrosis, inflammation, and tumorigenesis." *Cancer Cell* 10(1): 51-64.
- Desmarais, S., W. C. Black, et al. (2008). "Effect of cathepsin k inhibitor basicity on in vivo off-target activities." *Mol Pharmacol* 73(1): 147-56.
- Falgueyret, J. P., S. Desmarais, et al. (2005). "Lysosomotropism of basic cathepsin K inhibitors contributes to increased cellular potencies against off-target cathepsins and reduced functional selectivity." *J Med Chem* 48(24): 7535-43.
- Fehrenbacher, N. and M. Jaattela (2005). "Lysosomes as targets for cancer therapy." *Cancer Res* 65(8): 2993-5.
- Felbor, U., B. Kessler, et al. (2002). "Neuronal loss and brain atrophy in mice lacking cathepsins B and L." *Proc Natl Acad Sci U S A* 99(12): 7883-8.
- Glick, D., S. Barth, et al. (2010). "Autophagy: cellular and molecular mechanisms." *J Pathol* 221(1): 3-12.
- Hideo Sugita, Masaaki Kimura, et al. (1982). " In vivo administration of a thiol protease inhibitor, E-64-C, to hereditary dystrophic chicken " *Muscle and Nerve* 5(9): 738-744.

- Hoyer-Hansen, M., L. Bastholm, et al. (2005). "Vitamin D analog EB1089 triggers dramatic lysosomal changes and Beclin 1-mediated autophagic cell death." *Cell Death Differ* 12(10): 1297-309.
- Ikeda, H., T. Iehara, et al. (2002). "Experience with International Neuroblastoma Staging System and Pathology Classification." *Br J Cancer* 86(7): 1110-6.
- Isahara, K., Y. Ohsawa, et al. (1999). "Regulation of a novel pathway for cell death by lysosomal aspartic and cysteine proteinases." *Neuroscience* 91(1): 233-49.
- Kondo, Y., T. Kanzawa, et al. (2005). "The role of autophagy in cancer development and response to therapy." *Nat Rev Cancer* 5(9): 726-34.
- Kornfeld, S. (1992). "Structure and function of the mannose 6-phosphate/insulinlike growth factor II receptors." *Annu Rev Biochem* 61: 307-30.
- Levine, B. and D. J. Klionsky (2004). "Development by self-digestion: molecular mechanisms and biological functions of autophagy." *Dev Cell* 6(4): 463-77.
- Levy, J. M. and A. Thorburn (2011). "Targeting autophagy during cancer therapy to improve clinical outcomes." *Pharmacol Ther* 131(1): 130-41.
- London, W. B., R. P. Castleberry, et al. (2005). "Evidence for an age cutoff greater than 365 days for neuroblastoma risk group stratification in the Children's Oncology Group." *J Clin Oncol* 23(27): 6459-65.
- Maris, J. M. (2010). "Recent advances in neuroblastoma." *N Engl J Med* 362(23): 2202-11.
- Mason, R. W., G. D. Green, et al. (1985). "Human liver cathepsin L." *Biochem J* 226(1): 233-41.
- Mizushima, N. (2007). "Autophagy: process and function." *Genes Dev* 21(22): 2861-73.
- Mohamed, M. M. and B. F. Sloane (2006). "Cysteine cathepsins: multifunctional enzymes in cancer." *Nat Rev Cancer* 6(10): 764-75.
- Opipari, A. W., Jr., L. Tan, et al. (2004). "Resveratrol-induced autophagocytosis in ovarian cancer cells." *Cancer Res* 64(2): 696-703.

- Perez-Castrillon, J. L., F. Pinacho, et al. (2010). "Odanacatib, a new drug for the treatment of osteoporosis: review of the results in postmenopausal women." *J Osteoporos* 2010.
- Pillay, C. S., E. Elliott, et al. (2002). "Endolysosomal proteolysis and its regulation." *Biochem J* 363(Pt 3): 417-29.
- Rice, D. and S. Barone, Jr. (2000). "Critical periods of vulnerability for the developing nervous system: evidence from humans and animal models." *Environ Health Perspect* 108 Suppl 3: 511-33.
- Sajid, M., S. A. Robertson, et al. (2011). "Cruzain : the path from target validation to the clinic." *Adv Exp Med Biol* 712: 100-15.
- Shaw, E. (1994). "Peptidyl diazomethanes as inhibitors of cysteine and serine proteinases." *Methods Enzymol* 244: 649-56.
- Sloane, B. F., K. Moin, et al. (1994). "Membrane association of cathepsin B can be induced by transfection of human breast epithelial cells with c-Ha-ras oncogene." *J Cell Sci* 107 (Pt 2): 373-84.
- Stahl, S., Y. Reinders, et al. (2007). "Proteomic analysis of cathepsin B- and L-deficient mouse brain lysosomes." *Biochim Biophys Acta* 1774(10): 1237-46.
- Tjelle, T. E., A. Brech, et al. (1996). "Isolation and characterization of early endosomes, late endosomes and terminal lysosomes: their role in protein degradation." *J Cell Sci* 109 (Pt 12): 2905-14.
- Tsujimoto, Y. and S. Shimizu (2005). "Another way to die: autophagic programmed cell death." *Cell Death Differ* 12 Suppl 2: 1528-34.
- Turk, B., D. Turk, et al. (2000). "Lysosomal cysteine proteases: more than scavengers." *Biochim Biophys Acta* 1477(1-2): 98-111.
- Turk, V., B. Turk, et al. (2002). "Lysosomal cathepsins: structure, role in antigen processing and presentation, and cancer." *Adv Enzyme Regul* 42: 285-303.
- Van Noesel, M. M. and R. Versteeg (2004). "Pediatric neuroblastomas: genetic and epigenetic 'danse macabre'." *Gene* 325: 1-15.
- Vasiljeva, O. and B. Turk (2008). "Dual contrasting roles of cysteine cathepsins in cancer progression: apoptosis versus tumour invasion." *Biochimie* 90(2): 380-6.

Volchenboum, S. L. and S. L. Cohn (2009). "Progress in defining and treating high-risk neuroblastoma: lessons from the bench and bedside." *J Clin Oncol* 27(7): 1003-4.

Wagner, L. M. and M. K. Danks (2009). "New therapeutic targets for the treatment of high-risk neuroblastoma." *J Cell Biochem* 107(1): 46-57.

White, E. and R. S. DiPaola (2009). "The double-edged sword of autophagy modulation in cancer." *Clin Cancer Res* 15(17): 5308-16.

Xing, R., A. K. Addington, et al. (1998). "Quantification of cathepsins B and L in cells." *Biochem J* 332 (Pt 2): 499-505.

Xing, R., F. Wu, et al. (1998). "Control of breast tumor cell growth using a targeted cysteine protease inhibitor." *Cancer Res* 58(5): 904-9.

Yang, Z. J., C. E. Chee, et al. (2011). "The role of autophagy in cancer: therapeutic implications." *Mol Cancer Ther* 10(9): 1533-41.

Zhu, D. M. and F. M. Uckun (2000). "Cathepsin inhibition induces apoptotic death in human leukemia and lymphoma cells." *Leuk Lymphoma* 39(3-4): 343-54.

Zhu, D. M. and F. M. Uckun (2000). "Z-Phe-Gly-NHO-Bz, an inhibitor of cysteine cathepsins, induces apoptosis in human cancer cells." *Clin Cancer Res* 6(5): 2064-9.

SECTION 2: LEUKEMIA

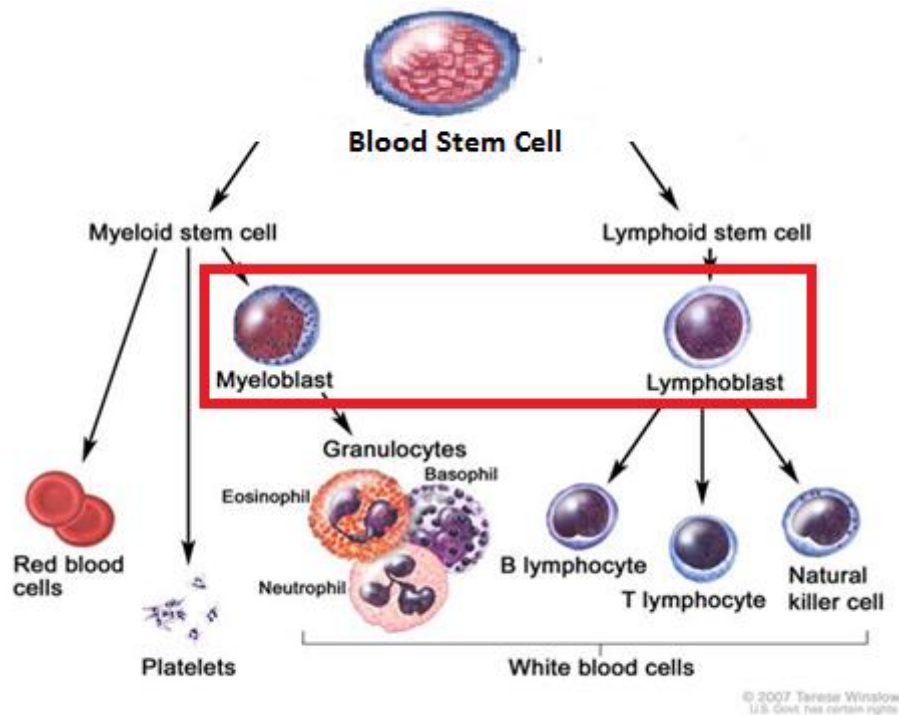
Chapter 5

INTRODUCTION

5.1 Leukemia

Leukemia is a cancer of the blood that originates in the bone marrow and the lymphatic system. The figure below (Figure 1.1) outlines the development of normal blood cells from a stem cell that originates in the bone marrow. The blood stem cell undergoes a series of differentiation steps to mature either into red blood cells (RBCs), platelets or any of the white blood cells (WBCs). The RBCs or erythrocytes supply oxygen and nutrients throughout the body via the circulatory system. The platelets or thrombocytes control excessive bleeding by formation of clots when injured. The WBCs or leukocytes strengthen the body's immune system to fight infections.

In majority of patients, leukemia occurs due to chromosomal aberrations in immature blood stem cells that originate in the bone marrow. This limits the normal process of differentiation that forms mature blood cells, essential for the daily functioning of the body. Consequently, the circulatory system is characterized by rapid proliferation of immature blasts that crowd out normal RBCs, platelets and WBCs. On this account, the patient may experience anemia, excessive bleeding in case of injury and could also succumb to infections due to a weakened immune system. Further, the accumulation of immature blasts to various sites in the body result in disease symptoms such as hepatosplenomegaly (enlarged spleen and liver), joint aches, headaches, or sixth-nerve palsy.



Adapted from <http://www.cancer.gov/cancertopics/pdq/treatment/childALL/Patient> - Accessed on 11/07/2013

Figure 5.1: Schematic representation of normal blood cell development

First, a stem cell matures into either a myeloid stem cell or a lymphoid stem cell:

- A myeloid stem cell matures into a myeloid blast. This blast cell undergoes further differentiation to form a red blood cell, platelets, or one of several types of white blood cells.
- A lymphoid stem cell matures into a lymphoid blast. The blast can form one of several types of white blood cells, such as B lymphocyte, T lymphocyte or Natural Killer cells.

Lymphoblastic leukemia is characterized by malignant proliferation of immature lymphoblasts, curbing the development of healthy blood cells. Under these pathological conditions, the bone marrow produces abnormal white blood cells, which

crowd out normal white blood cells, red blood cells, and platelets and prevent the normal functions to be carried on. The proliferation of these malignant cells leads to massive infiltration of immature lymphoblasts to various sites in the body including the lymphoid system, liver and spleen (hepatosplenomegaly); and the central nervous system.

5.2 Types of Leukemia

The classification of the types of leukemia is based on how rapidly the disease progresses and the type of blood cells that are affected. Based on this categorization leukemia can be acute or chronic. Acute leukemia is a condition where the abnormal blood cells remain immature and cannot carry out their normal functions. The number of blasts increases rapidly, and the disease progresses quickly. In chronic leukemia, the cells are more mature and can carry out some of their normal functions. The number of blasts increases less rapidly compared to that of acute leukemia. In this condition the disease worsens gradually. Leukemia can arise in either of the two main types of white blood cells — lymphoid cells or myeloid cells. When leukemia affects lymphoid cells, it is called lymphocytic leukemia. When myeloid cells are affected, the disease is called myeloid or myelogenous leukemia. The disease appears in one of four major forms:

Acute lymphocytic leukemia (ALL)

ALL affects lymphoid cells and grows quickly. ALL is the most common type of leukemia in young children and adults; especially adults age 65 and older.

Acute myeloid leukemia (AML)

AML affects myeloid cells and grows quickly. It occurs in both adults and children. This type of leukemia is sometimes called acute nonlymphocytic leukemia (ANLL).

Chronic lymphocytic leukemia (CLL)

CLL affects lymphoid cells and usually grows slowly. Most often, people diagnosed with the disease are over age 55. It sometimes occurs in younger adults, but it almost never affects children.

Chronic myeloid leukemia (CML)

CML affects myeloid cells and usually grows slowly at first. It mainly affects adults, although a very small number of children also develop this disease.

5.3 Incidence Rates of Leukemia

An estimated 52,380 new cases of leukemia are expected to be diagnosed in the US in 2014. Cases of acute leukemia are expected to account for 14.7 percent more cases than chronic leukemia. ALL accounts for 76% of all childhood and adolescent leukemia with incidence rates that peak at the age of 5 years.

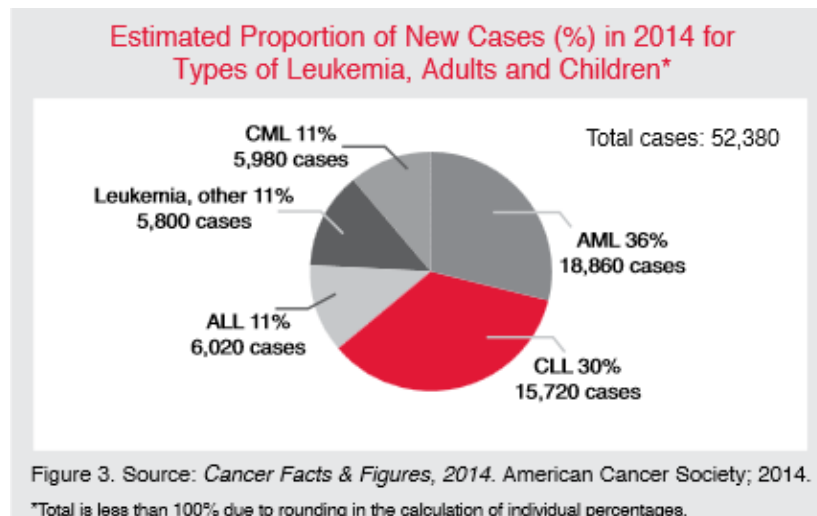


Figure 5.2: Proportion of new cases for the types of leukemia in adults and children 2014

In 2014, leukemia is expected to strike approximately 12 times as many adults (47,666) as children and adolescents younger than 20 years (4,103). Leukemia is the most common cancer in children and adolescents less than 20 years old. About 32 percent of estimated cancer cases in children and adolescents younger than 15 years are leukemia. ALL is the most common cancer in children 1 to 7 years old. The incidence of ALL among 1- to 4-year-olds is nearly eight times greater than the rate for young adults 20 to 24 years. Incidence of ALL is higher in children and adolescents younger than 15 years. AML incidence is lower in children and adolescents from 1 to 14 years.

Total Estimated Number of New Leukemia Cases in the United States for 2014			
Type	Total	Male	Female
Acute Lymphoblastic Leukemia	6,020	3,140	2,880
Chronic Lymphocytic Leukemia	15,720	9,100	6,620
Acute Myeloid Leukemia	18,860	11,530	7,330
Chronic Myeloid Leukemia	5,980	3,130	2,850
Other Leukemia	5,800	3,200	2,600
Total Estimated New Cases	52,380	30,100	22,280

Table 3. Source: *Cancer Facts & Figures 2014*. American Cancer Society; 2014.

Table 5-1: Number of new leukemia cases in the United States 2014

5.4 Current Therapies for Leukemia

Many factors play an important role in the treatment of leukemia. Some of the factors include age and overall health, the type of leukemia, and whether the disease has spread to other parts of the body. Some of the commonly available treatment options are listed below.

Chemotherapy

The most common form of treatment for leukemia is chemotherapy. In this form of treatment chemical compounds are used to destroy leukemic cells. Single drug or a combination of drugs may be used to treat the patient depending on the type of leukemia the patient is diagnosed with. Some of the commonly used drugs are asparaginase, clofarabine, daunorubicin, doxorubicin, methotrexate, nelarabine, or vincristine and corticosteroids (dexamethasone or prednisone). These drugs may be ingested orally or injected directly into a vein.

Biological therapy

Biological therapy is a process by which the body's defense mechanism is stimulated to protect against the disease by recognizing and attacking the leukemic cells. For example, monoclonal antibodies which specifically target proteins over expressed in leukemic cells. Another type of monoclonal antibody carries the toxin that selectively kills the leukemic cells. Interferon is a part of a family of proteins called cytokines which attach to other immune cells, activating them to help the body fight infections and tumors. Man-made versions of these substances are sometimes used as a form of immunotherapy. Interferon is used in CML patients which slows the growth of leukemic cells.

Targeted therapy

In this type of treatment the drugs attack certain susceptible characteristics of the cancer cells. They aid in blocking the growth of the leukemic cells. An example for targeted therapy that blocks the action of an abnormal protein which helps in the growth of the leukemic cells is the drug imatinib (Gleevec). This drug is used in patients with CML.

Radiation therapy

X-rays and other high beam radiation is used to damage the leukemic cells and prevent their growth. During this form of therapy, the high energy beams are directed to specific points of the body where there is an accumulation of leukemic cells or may receive radiation throughout the body. Radiation therapy kills cancer cells by damaging their DNA. It can either damage DNA directly or create charged particles within the cells that can in turn damage the DNA. Cancer cells whose DNA is damaged beyond repair stop dividing or die. When the damaged cells die, they are broken down and eliminated by the body's natural processes.

Stem cell transplant

This is a procedure where the diseased bone marrow is replaced by a healthy one. High doses of chemotherapy or radiation therapy are given to the patient to destroy both leukemia cells and normal blood cells in the bone marrow before the start of the stem cell transplant. Once this is done the patient is infused with new stem cells from a healthy donor to replace the diseased bone marrow.

5.5 Preclinical Mouse Models of Leukemia

Animal disease models are the primary vehicles to determine efficacy and toxicities of potential cancer chemotherapeutic agents before entering clinical trials. Different animal models for various malignant diseases have been developed as a result. These animal models are divided into two groups : 1) grafts of tumor material (syngeneic or xenogeneic) into immunocompetent or immunodeficient animals, respectively and 2) genetically engineered mice that mimic a specific cancer genotype. These animal disease models can be used to identify and validate several novel

compounds for the treatment of various diseases. Scid/scid mice are severely deficient in functional B and T lymphocytes since the mutation appears to impair the recombination of antigen receptor genes and causes an arrest in the early development of B and T lineage-committed cells whereas other hematopoietic cell types appear to develop and function normally (M J Bosma, and A M Carroll 1991). These mice were used in many studies to carry out efficient transplantation and propagation of human tumor tissues as xenografts. These xenograft mouse models allow the in vitro human cell lines to be propagated thereby recapitulating the disease. Another difficulty faced during the development of mouse models is the graft-versus-host disease (GVHD) that may occur when they receive donated cells (Gerard Socié and Bruce R. Blazar 2009). In GVHD, the donated white blood cells in the stem cell graft react against the mouse's normal tissues. Most often, the liver, skin, or digestive tract is affected. In order to overcome the threat of graft rejection during the transplantation of human hematopoietic cells into these recipients, immuno-compromised (SCID) mice are used. It has been reported in earlier studies that leukemia cell lines and primary patient cells have been engrafted into SCID mice leading to leukemia manifestation similar to the patient's disease (Lüder H. Meyer et al 2011). However, the residual immunity of SCID mice does seem to limit efficiency of xenografting in these mice. In our study we used NSG-B2m (NOD.CgPrkdc^{scid} B2m^{tm1Unc} Il2rg^{tm1Wjl}/SzJ) mice. These triple mutant mice have the severe combined immune deficiency mutation (scid), IL2 receptor gamma chain (IL2 γ) deficiency, and a MHC class I molecule (beta-2 microglobulin) deficiency. These mice are generally resistant to graft versus host disease (GVHD). Earlier studies showed that NOD-scid IL2 γ null mice lack host NK cells, thereby aiding in human peripheral blood mononuclear cells (PBMC)

engraftment. However, although IL2 receptor gamma chain deficiency improved survival and function of engrafted human T cells, severe xenogeneic GVHD developed following engraftment into these NK cell-deficient hosts. MHC class I molecule deficiency was shown to greatly reduce human *in vitro* T cell proliferative responses to murine cells and also lead to reduced development GVHD following engraftment (Steve Pino et al 2010). Thus the triple mutant NSG-B2m mice provide a model useful to study *in vivo* mechanisms of xenogeneic GVHD and to rapidly assess therapeutic agents. In this study, I show that transplantation of primary acute lymphoblastic leukemia (ALL) cells into NSG-B2m recipients leads to a leukemia model that resembles the distribution and course of the human disease.

Chapter 6

MATERIALS AND METHODS

6.1 Cell Lines and Culture

RS4;11 (established from an ALL patient) and Nalm6 (established from a patient with ALL at relapse) cell lines were purchased from the American Type Culture Collection (ATCC, Manassas, VA). Cells were maintained in RPMI media (Life Technologies) supplemented with 20% fetal bovine serum (FBS), glutamine, and penicillin/streptomycin. All cells were maintained at 37°C under a humidified atmosphere of 95% air and 5% CO₂.

6.2 Leukemia Cells from Patient Samples

Mononuclear cells from bone marrow aspirates from pediatric ALL patients treated at Nemours were obtained from Nemours Biobank in accordance with Institutional Review Board-approved protocol. Mononuclear cells were purified on a Ficoll density gradient and cryopreserved in liquid nitrogen in the presence of 10% dimethyl sulfoxide (DMSO) until required. Prior to transplantation, cells were thawed rapidly in RPMI1640 medium (Life Technologies) containing 10% FBS. After centrifugation at 250g for 5 minutes at 4°C, cells were resuspended in RPMI 1640 containing 10% FBS, and the number of viable cells estimated by exclusion of 0.2% trypan blue. Cells were recentrifuged, resuspended in ice-cold calcium- and magnesium-free phosphate-buffered saline (PBS), and placed on ice until inoculation into mice.

6.3 Engraftment of Human Leukemia Cells into NSG B2m Mice

All experimental procedures involving NSG-B2m mice were approved by the Nemours/AI duPont Animal Care and Use Committee (IACUC). Female NSG B2m mice aged 5 to 6 weeks were purchased from the Jackson Laboratories and housed in a specific pathogen-free environment for at least 1 week prior to inoculation with human leukemia cells. Mice were supplied with sterile food, water and bedding. Immediately prior to inoculation, mice were warmed by infrared lamp, then inoculated by tail-vein injection with between 2.5 and 10 million leukemia cells in a maximum volume of 100 μ L PBS. Mice were returned to their cages and examined daily and weighed weekly for general well-being.

To monitor leukemic progression, 50- μ L peripheral blood samples was drawn by sub-mandibular bleeding (Golde WT et al 2005). This method of bleeding is done with precision and practice. There is a small vascular bundle at the back of the jaw characterizes the cheek of laboratory mice (Fig. 6.1). It is at this point where the orbital veins, the submandibular vein, and other veins merge to form the beginning of the jugular vein. The animal is held by the scruff of the neck to ensure the most relaxed situation for the mouse. Using a scalpel number 11, the cheek of the mouse is poked with enough force to small stick hole for the blood to exude from the point of penetration. The blood is collected in eppendorf tubes containing 20 μ L of sodium citrate which acts as an anti-coagulant. To obtain sufficient blood, the position of the punch is crucial. About 0.7ml of blood can be collected from an adult mouse by this technique. The bleeding can be stopped by pressing down the wound using a sterile gauze.

At the first indication of weight loss, lethargy, ruffled fur, or no more than 28 weeks following inoculation, mice were euthanized. Cell suspensions of spleens and

other organs were prepared by mincing the tissues and filtering through 70 um cell strainers. Bone marrow was collected by flushing femurs with RPMI 1640 containing 10% FBS. Mononuclear cells were purified by density gradient centrifugation, and cells were cryopreserved in FBS containing 10% DMSO.



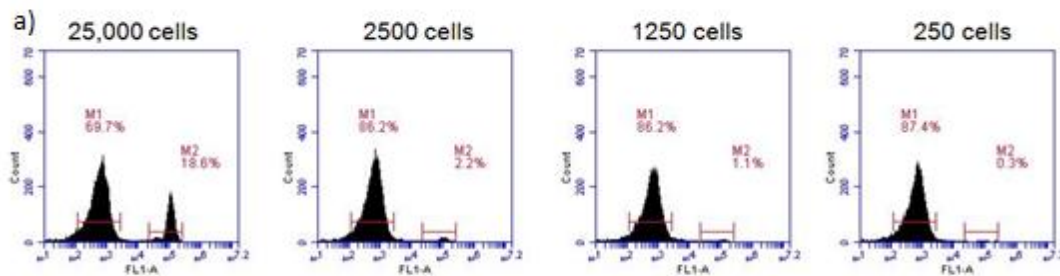
Figure 6.1: Sub-mandibular bleeding in mice.

The above figure shows the two veins - the retro-orbital and sub mandibular veins at a point where they merge at the origin of the jugular vein.

6.4 Monitoring of Leukemic Cells After Engraftment and Flow Cytometric Analysis

For flow cytometric analysis of blood samples, erythrocytes were lysed using NH_4Cl , and the remaining cells were washed in phosphate-buffered saline supplemented with 1% human albumin. The percentage of human cells (%Hu) in blood, spleen, and bone marrow was determined by double staining of the samples

with fluorescein isothiocyanate (FITC)–conjugated antimurine and allophycocyaninconjugated antihuman CD45 (BD Pharmingen, San Diego, CA)(Bart A Nijmeijer et al 2001). Samples were analyzed on a Accuri C6 flow cytometer. Total lymphoblasts (mouse and human) were gated on the basis of their forward and sideward light scattering properties. RS4;11 cells mixed with 50µl mouse peripheral blood were used to standardize the flow cytometer to detect human cells in mouse peripheral blood. The mixture of cells was stained with FITC-conjugated anti-human CD45 antibody and analyzed by flow cytometry. The first peak in Figure 6.2a represents unstained mouse peripheral blood monocytes while the second peak depicts the FITC stained RS4;11 cells. The graphs represent a range of RS4;11 cell dilutions from 25,000 to 250 cells. Detection as low as 0.3% RS4;11 cells in mouse blood was possible by flow cytometry. Figure 6.2b shows a plot of number of RS4;11 cells as a percentage of FITC positive cells over negative cells. A perfect correlation between these two variables was observed confirming the sensitivity of this technique.



b)

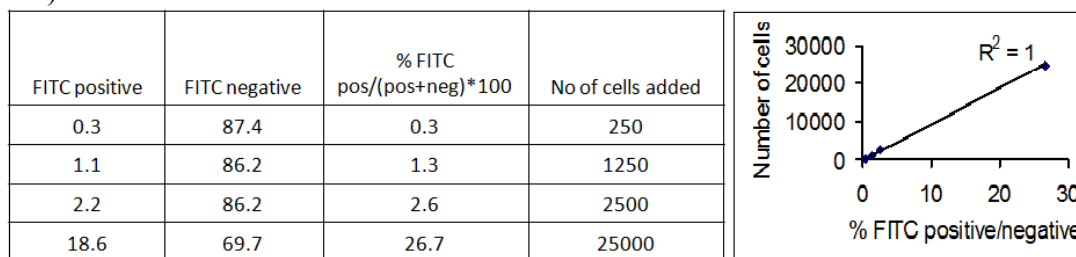


Figure 6.2:Intravenous transfer of ALL cells.

In (a) flow data of events versus FITC fluorescence with a fixed volume of mouse blood mixed with decreasing numbers of human cells are shown. In (b) the numbers of RS4;11 cells added to mouse blood in relation to percentage of FITC positive cells (human) in total cell population (mouse + human) are shown in table and graphical format.

Chapter 7

RESULTS

7.1 Engraftment of Primary Childhood ALL Cells

Mice were intravenously injected with $5-10 \times 10^6$ mononuclear ALL cells (Nalm6, RS4;11, or primary ALL cells). Flow cytometric analysis of peripheral blood samples with fluorescein isothiocyanate (FITC)-conjugated antimurine and allophycocyanin conjugated antihuman antibodies were used to monitor disease progression. The leukemic cells from the patients engrafted in NSG-B2m mice, although different progression rates were observed, following which the leukemic cell counts increased exponentially. The rate of engraftment of immortalized cell lines was faster than that for the primary ALL cells. In this study, we evaluated engraftment and progression of primary childhood ALL cells (Nalm6 and RS4;11) and two patient samples transplanted into NSG-B2m mice which appear to provide an accurate representation of the human disease.

Sample	Age	Sex	Genomic Abnormality	Type of Leukemia
NTPL-20	6yr	M	t(9;22)	B-ALL
NTPL-24	4yr	M	6q deletion	T-ALL

Table 7-1: Patient samples used in development of xenograft mouse model for leukemia

The NSG-B2m model reveals important biologic characteristics of childhood ALL that may ultimately be used to predict relapse and design novel treatment strategies.

7.2 Analysis of Engraftment and Progression of ALL Cells

Once the cells were inoculated, the mice were kept under observation. In order to study the progression of the disease, 50 μ L peripheral blood was drawn by sub-mandibular bleeding (Golde WT et al 2005). Blood was drawn at regular intervals (weekly or biweekly depending on the growth rate) to monitor the progression of the disease. The blood samples were then treated with human CD45-FITC and mouse CD45-APC antibodies which are specific for staining leukocytes in order to differentiate the human from the mouse cells. Based on the preliminary standardization of flow cytometry, the mouse and human cells were gated on a scatter plot and were distinguished by species- specific antibody staining. Each blue dot represents a single mouse cell, while a red dot represents a human cell.

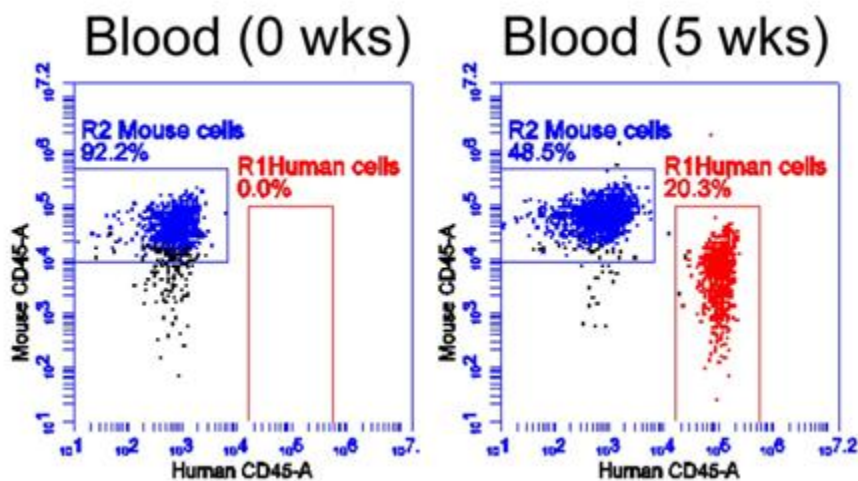


Figure 7.1: Engraftment and progression of human ALL cells in peripheral blood.

In the above figure, the engraftment and progression of human leukocytes is measured in peripheral blood inoculated with RS4;11 cells is shown. Note that no human cells were detected before injection (0 weeks).

7.3 Analysis of Leukemic Distribution in Other Organs

To establish the distribution of the engrafted ALL cells in other organs, the mice were injected with 10^7 RS4;11 cells. At various intervals, peripheral blood was sampled. Five weeks after cell injection, mice were sacrificed, and bone marrow and spleen cell suspensions were prepared and analyzed. The detected levels of leukemic engraftment in the tissues are shown in Figure 7.2.

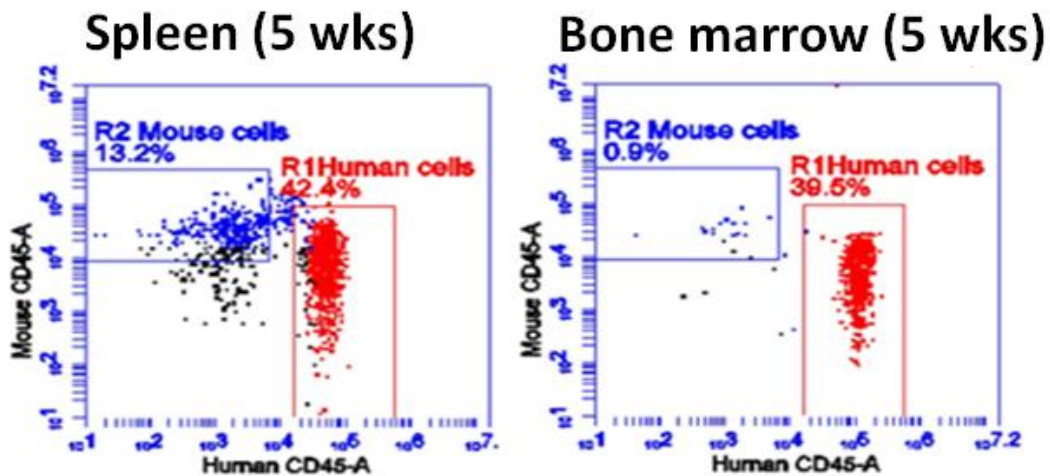


Figure 7.2: Engraftment and progression of human leukocytes measured in spleen and bone marrow.

In the above figure, the engraftment of human leukocytes measured in spleen and bone marrow 5 weeks post inoculation with RS4;11 cells is shown.

7.4 Enlarged Leukemic Spleen when compared to Normal Spleen

Around four weeks after injection, infiltration of the ALL cells is seen in the mouse bone marrow, spleen, and peripheral blood. The leukemic cells once engrafted into to the bone marrow within a couple of weeks appeared in the peripheral blood (Lock RB et el 2002). Late stages of engraftment will cause accumulation of ALL cells within the spleen, thereby resulting in an enlarged spleen as seen in Figure 7.3.



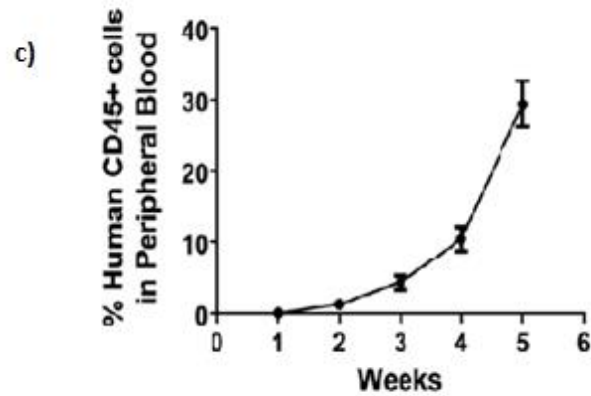
Figure 7.3: Comparison of a leukemic spleen to a normal spleen.

The above figure shows the later stages of engraftment which leads to accumulation of leukemic cells thereby causing spleen enlargement when compared with that of a normal mouse.

7.5 Leukemia Progression in the Mouse Model

RS4;11 cells (5×10^6) were injected into the tail vein of female NSG-B2m mice (6–8 weeks old; 7/group). Weekly sub-mandibular bleeding was used to monitor disease progression as described above (section 6.3). The time delay to engraftment

was demonstrated by the initial lag phase, which varied between different cell lines, prior to exponential increase in the proportion of human CD45⁺ cells in the peripheral blood. Progression of the disease is shown in Figure 7.4. Figure 7.4 b) shows an infected mouse suffering from hind limb paralysis which is due to the invasion by malignant cells from vertebral body marrow cavities into the spinal canal. At harvest, bone marrow, spleens, and peripheral blood had high levels of human CD45⁺ cells where the bone marrow and spleen mouse CD45⁺ cells were almost replaced by the human leukocytes (Figure 7.2). Figure 7.4 c) and d), shows the gradual increase in the human cells in the peripheral blood.



d)

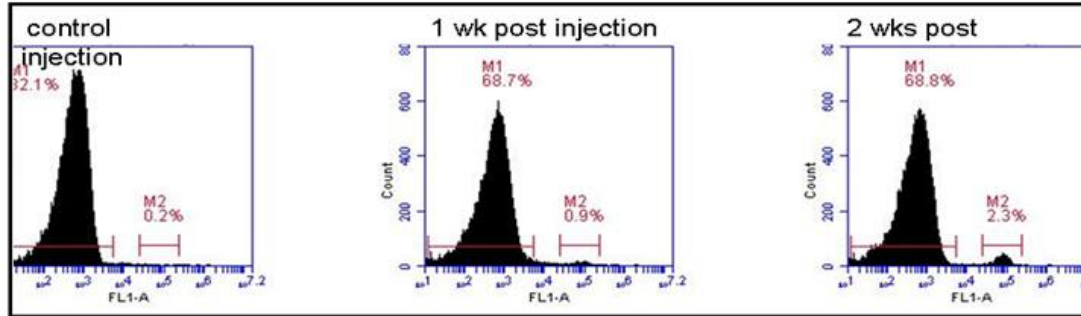


Figure 7.4: a) normal mouse b) mouse infected with leukemic cells c) Graph representing leukemic progression d) Leukemic progression shown in flow cytometry.

7.6 Serial Transplantation of Leukemic Cells in NSG-B2m Mice

Mononuclear cells were purified from the spleens of engrafted animals by density gradient centrifugation (Figure 7.5a) and cryopreserved. Serial transplants were carried out by inoculation of cells that were thawed and processed exactly as described above for primary cells. Equal numbers of human leukemia cells were inoculated in each case. This study was mainly carried out to determine whether the leukemia could be transferred to secondary and tertiary recipients, and whether proliferation rates changed over repeated passaging. The engraftment rates of the primary and spleen derived cells were similar (Figure 7.5b).

a)



b)

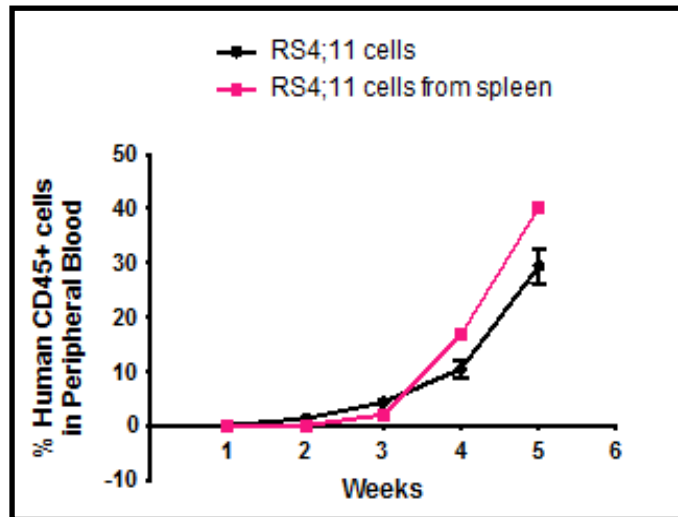


Figure 7.5: a) Ficoll Gradient showing the separated layer of leukocytes from a spleen sample. b) Graphical representation showing similar engraftment rates in serial transplantation.

Chapter 8

DISCUSSION

Development of a mouse model by engraftment of human leukemia cells requires prevention of immune rejection of the human cells and reaction of the engrafted cells against host cells. Previous studies have shown that hemopoietic stem cells can be engrafted in NOD-scid mice. Engraftment was improved by development of NOD-scid mice homozygous for a targeted mutation in the 2-microglobulin structural gene (NOD-scid B2m null mice). These mice had severely deficient NK cell activity and the levels of engraftments were higher. However, these mice had a shortened life span due to accelerated thymic lymphoma genesis (Christianson, S. W., et al 1997). Other immuno deficient mouse models have been developed with targeted mutation in the recombination activation gene 1 (NOD-Rag1^{null}). These mice had an increased life span but faced challenges but engrafted cells failed to differentiate into mature human lymphoid and myeloid cells (Shultz, L. D.,et al 2003). Another significant mouse model that was developed for human hemopoietic stem cells engraftment was the *IL2Rg*^{null} mouse. These animals lack mature lymphocytes and NK cells, express other severe impairments in innate immunity, do not develop thymic lymphomas, and are long-lived (Shultz, L. D et al 2005).

In this study we used NSG-B2m(NOD.CgPrkdc^{scid} B2m^{tm1Unc} Il2rg^{tm1Wjl}/SzJ) mice which do not express the Prkdc gene, the X-linked Il2rg gene nor the B2m gene. They are triple mutant mice with combined features of severe combined immune deficiency mutation, significantly faster development of leukemia related symptoms

than other models, and higher percentage of leukemic cells in the blood, marrow and the spleen (Alice Agliano et al 2008). The NSG-B2m mice were reported to have increased mean survival time of about 44 days which when compared to the NOD-scid Il2ry^{null} is around 21 days. In this model, the animals did not undergo irradiation as done in previous studies to wipe out the host bone marrow prior to injection of leukemic cells. This animal disease model has been used to test novel therapies or to examine the efficacy of drugs used in the treatment of childhood ALL (Lock RB et al 2002). Animal disease models are developed either by using xenografts established as systemic disease by intravenous or intraperitoneal inoculation of leukemia cells or localized leukemia growth following subcutaneous or intraocular injections. Developing a subcutaneous xenograft model is considered convenient, faster and less expensive. The anti tumor activity of testing various compounds can be established by measuring the tumor size. One of the major advantages of the subcutaneous xenograft model is that they are easily accessible to the tumor and aid in facilitating objective measurements. They are straightforward to implant and are palpable (Daisuke Sano et al 2009). However in comparison with subcutaneous xenograft models, the orthotopic xenograft models are advantageous for their ability to mimic local tumor microenvironment that leads to development of tumor cells with the biological and metastatic properties similar to clinical cases, thereby leading to more reliable translation to the human disease (Nutritional Oncology by George L. Blackburn 2006). The majority of the studies used the model where ALL is established as a systemic disease to monitor the effects of the drugs or for novel therapies. Some of the notable characteristics of the model used in this study that may be advantageous for preclinical testing of new therapies include developing continuous xenografts from patients who

underwent diverse treatment results, propagation as models of systemic disease, retention of the fundamental biologic characteristics of the original disease, ability to monitor engraftment and response to therapy and giving a spectrum of sensitivity to established drugs providing an overall reflection of patient outcome (Natalia L. M. Liem. et al 2004)

Previous studies in our laboratory have shown that NSG-B2m mice are an ideal animal model that supports the highly efficient engraftment of ALL cell lines (Krishnan et al 2013). In this study I have extended this work to show that cells obtained directly from patients engraft successfully in this animal disease model. Efficient engraftment was achieved by using just 5×10^6 primary childhood ALL cells. The time course of appearance of human CD45 + cells in the mouse peripheral blood depicts the pathogenicity of the disease seen in patients. We showed that ALL cells from children could be passaged in NSG B2m mice for at least 3 cycles, providing a reliable and robust representation of the human disease. The initial lag phase followed by exponential growth is characteristic of the time required for injected cells to home to the bone marrow, proliferate to replace the normal bone marrow architecture, and then disseminate to the peripheral blood and other organs.

The ultimate goal of this study is to investigate the cause of childhood ALL and thereby improve treatment outcomes. This animal disease model provides critical features of leukemia biology that can be used to characterize the pathophysiology of leukemic growth and progression, and to determine therapeutic modalities of treatment regimens. Our demonstration of efficient and high-level engraftment of primary ALL cells from patients without host pre-conditioning, indicates that a wide range of

different leukemias can be used to identify therapeutics that are likely to be effective against a range of patients.

REFERENCES

(Leukemia)

- Agliano, A., I. Martin-Padura, et al. (2008). "Human acute leukemia cells injected in NOD/LtSz-scid/IL-2Rgamma null mice generate a faster and more efficient disease compared to other NOD/scid-related strains." *Int J Cancer* 123(9): 2222-7.
- Baersch, G., T. Mollers, et al. (1997). "Good engraftment of B-cell precursor ALL in NOD-SCID mice." *Klin Padiatr* 209(4): 178-85.
- Bosma, M. J. and A. M. Carroll (1991). "The SCID mouse mutant: definition, characterization, and potential uses." *Annu Rev Immunol* 9: 323-50.
- Cesano, A., R. O'Connor, et al. (1991). "Homing and progression patterns of childhood acute lymphoblastic leukemias in severe combined immunodeficiency mice." *Blood* 77(11): 2463-74.
- Christianson, S. W., D. L. Greiner, et al. (1997). "Enhanced human CD4+ T cell engraftment in beta2-microglobulin-deficient NOD-scid mice." *J Immunol* 158(8): 3578-86.
- Dick, J. E. (1996). "Normal and leukemic human stem cells assayed in SCID mice." *Semin Immunol* 8(4): 197-206.
- Dick, J. E., T. Lapidot, et al. (1991). "Transplantation of normal and leukemic human bone marrow into immune-deficient mice: development of animal models for human hematopoiesis." *Immunol Rev* 124: 25-43.
- Golde, W. T., P. Gollobin, et al. (2005). "A rapid, simple, and humane method for submandibular bleeding of mice using a lancet." *Lab Anim (NY)* 34(9): 39-43.
- Goldin, A., J. M. Venditti, et al. (1981). "Current results of the screening program at the Division of Cancer Treatment, National Cancer Institute." *Eur J Cancer* 17(2): 129-42.

- Houghton, P. J., C. L. Morton, et al. (2007). "The pediatric preclinical testing program: description of models and early testing results." *Pediatr Blood Cancer* 49(7): 928-40.
- Imada, K., A. Takaori-Kondo, et al. (1996). "Serial transplantation of adult T cell leukemia cells into severe combined immunodeficient mice." *Jpn J Cancer Res* 87(9): 887-92.
- Kamel-Reid, S., M. Letarte, et al. (1989). "A model of human acute lymphoblastic leukemia in immune-deficient SCID mice." *Science* 246(4937): 1597-600.
- Krishnan, V., X. Xu, et al. (2013). "Dexamethasone-loaded block copolymer nanoparticles induce leukemia cell death and enhance therapeutic efficacy: a novel application in pediatric nanomedicine." *Mol Pharm* 10(6): 2199-210.
- Liem, N. L., R. A. Papa, et al. (2004). "Characterization of childhood acute lymphoblastic leukemia xenograft models for the preclinical evaluation of new therapies." *Blood* 103(10): 3905-14.
- Lock, R. B., N. Liem, et al. (2002). "The nonobese diabetic/severe combined immunodeficient (NOD/SCID) mouse model of childhood acute lymphoblastic leukemia reveals intrinsic differences in biologic characteristics at diagnosis and relapse." *Blood* 99(11): 4100-8.
- Lucking-Famira, K. M., P. T. Daniel, et al. (1994). "APO-1 (CD95) mediated apoptosis in human T-ALL grafted in SCID mice." *Leukemia* 8(11): 1825-33.
- McGuirk, J., Y. Yan, et al. (1998). "Differential growth patterns in SCID mice of patient-derived chronic myelogenous leukemias." *Bone Marrow Transplant* 22(4): 367-74.
- Morton, C. L. and P. J. Houghton (2007). "Establishment of human tumor xenografts in immunodeficient mice." *Nat Protoc* 2(2): 247-50.
- Nijmeijer, B. A., P. Mollevanger, et al. (2001). "Monitoring of engraftment and progression of acute lymphoblastic leukemia in individual NOD/SCID mice." *Exp Hematol* 29(3): 322-9.
- Oehler, V. G., J. P. Radich, et al. (2005). "Randomized trial of allogeneic related bone marrow transplantation versus peripheral blood stem cell transplantation for chronic myeloid leukemia." *Biol Blood Marrow Transplant* 11(2): 85-92.

Peterson, J. K. and P. J. Houghton (2004). "Integrating pharmacology and in vivo cancer models in preclinical and clinical drug development." *Eur J Cancer* 40(6): 837-44.

Pino, S., M. A. Brehm, et al. (2010). "Development of novel major histocompatibility complex class I and class II-deficient NOD-SCID IL2R gamma chain knockout mice for modeling human xenogeneic graft-versus-host disease." *Methods Mol Biol* 602: 105-17.

Rombouts, W. J., A. C. Martens, et al. (2000). "Identification of variables determining the engraftment potential of human acute myeloid leukemia in the immunodeficient NOD/SCID human chimera model." *Leukemia* 14(5): 889-97.

Sano, D. and J. N. Myers (2009). "Xenograft models of head and neck cancers." *Head Neck Oncol* 1: 32.

Schmitz, N., M. Beksac, et al. (2005). "Filgrastim-mobilized peripheral blood progenitor cells versus bone marrow transplantation for treating leukemia: 3-year results from the EBMT randomized trial." *Haematologica* 90(5): 643-8.

Shultz, L. D., S. Banuelos, et al. (2003). "NOD/LtSz-Rag1nullPfpnull mice: a new model system with increased levels of human peripheral leukocyte and hematopoietic stem-cell engraftment." *Transplantation* 76(7): 1036-42.

Shultz, L. D., B. L. Lyons, et al. (2005). "Human lymphoid and myeloid cell development in NOD/LtSz-scid IL2R gamma null mice engrafted with mobilized human hemopoietic stem cells." *J Immunol* 174(10): 6477-89.

Socie, G. and B. R. Blazar (2009). "Acute graft-versus-host disease: from the bench to the bedside." *Blood* 114(20): 4327-36.

Uckun, F. M. (1996). "Severe combined immunodeficient mouse models of human leukemia." *Blood* 88(4): 1135-46.

Uckun, F. M., H. N. Sather, et al. (1998). "Prognostic significance of B-lineage leukemic cell growth in SCID mice: a Children's Cancer Group Study." *Leuk Lymphoma* 30(5-6): 503-14.

Uckun, F. M., B. J. Waurzyniak, et al. (1999). "Prognostic significance of T-lineage leukemic cell growth in SCID mice: a Children's Cancer Group study." *Leuk Lymphoma* 32(5-6): 475-87.

Wang, J. C., T. Lapidot, et al. (1998). "High level engraftment of NOD/SCID mice by primitive normal and leukemic hematopoietic cells from patients with chronic myeloid leukemia in chronic phase." *Blood* 91(7): 2406-14.

White, L., A. Trickett, et al. (1990). "Heterotransplantation of human lymphoid neoplasms using a nude mouse intraocular xenograft model." *Cancer Res* 50(10): 3078-86.

Yan, Y., O. Salomon, et al. (1996). "Growth pattern and clinical correlation of subcutaneously inoculated human primary acute leukemias in severe combined immunodeficiency mice." *Blood* 88(8): 3137-46.

Appendix A

IACUC LETTER OF APPROVAL



Institutional Animal Care and Use Committee

MEMORANDUM

DATE: July 26, 2013
TO: Robert Mason, PhD
FROM: Paul T. Fawcett, Ph.D. 
SUBJECT: Mouse model of neuroblastoma treatment

The Institutional Animal Care and Use Committee (IACUC) have reviewed the full protocol submission on the above referenced project and the following decision has been made:

Action: Approved

Date of Action: July 26, 2013

Approval Period: July 26, 2013 to July 25, 2014

Protocol Approval Number: NBR-2013-004

Approved Number of Animals: Mouse SCID 60

Please submit your Biosafety Classification form electronically to the Alfred I. duPont Hospital for Children Institutional Biosafety Committee via the link:

<http://www.nemours.org/research/committee/ibc.html>

Please note that the study cannot begin until the Office of Regulatory Compliance in Research Administration has received all approvals.

Please maintain this approval with your project records. A tally of the number of animals approved and the number ordered for the project will be maintained in the Life Science Center. If changes occur in your protocol or if you require more animals than approved, and amendment to your protocol will need to be submitted for consideration

If you have any questions regarding this memorandum, please contact Paul T. Fawcett, Ph.D. at x 6776 or email: pfawcett@nemours.org.

Appendix B

IACUC LETTER OF APPROVAL



Institutional Animal Care and Use Committee

MEMORANDUM

DATE: November 27, 2012
TO: Sonali Barwe, Ph.D.
FROM: Paul T. Fawcett, Ph.D.
SUBJECT: "The role of annexin II in cell survival and drug resistance in a mouse model of acute lymphoblastic leukemia" NBR-2009-007

The Institutional Animal Care and Use Committee (IACUC) have reviewed the above referenced protocol for approval, and the following decision has been made:

Action: Renewal Approved

Date of Action: November 27, 2012

Approval Period: November 27, 2012 – November 26, 2013

Protocol Approval Number: NBR-2009-007

Approved Number of Animals: NOD/SCID or NSG-B2m 895

Please submit your Biosafety Classification form electronically to the Alfred I. duPont Hospital for Children Institutional Biosafety Committee via the link:

<http://www.nemours.org/research/committee/ibc.html>

Please note that the study cannot begin until the Office of Regulatory Compliance in Research Administration has received all approvals.

Please maintain this approval with your project records. A tally of the number of animals approved and the number ordered for the project will be maintained in the Life Science Center. If changes occur in your protocol or if you require more animals than approved, and amendment to your protocol will need to be submitted for consideration

If you have any questions regarding this memorandum, please contact Paul T. Fawcett, Ph.D. at x 6776 or email: pfawcett@nemours.org.

Appendix C

IRB LETTER OF APPROVAL



Nemours Office of Human Subjects Protection
10140 Centurion Parkway North
Jacksonville, FL 32256
Phone: 904-697-4023 Fax: 904-697-4024

MEMORANDUM

DATE: October 3, 2011

TO: E. Anders Kolb, MD

FROM: Nemours Delaware IRB

STUDY TITLE: [267207-1] Establishment of Xenograft Models of Pediatric Leukemia Utilizing Tumor Bank Specimens

IRB #: 267207

SUBMISSION TYPE: New Project

ACTION: EXEMPT

DECISION DATE: September 29, 2011

Thank you for your submission of New Project Materials for the above referenced study. Your submission received Expedited Review based upon the applicable federal regulations and meets all DHHS criteria for Exemption.

The IRB determined that:

The research is exempt from further IRB review based upon the applicable federal regulations 45CFR46.101(b) under Category 4.

Exempt Category 4. Research, involving the collection or study of existing data, documents, records, pathological specimens, or diagnostic specimens,

- If these sources are publicly available or
- If the information is recorded by the investigator in such a manner that subjects cannot be identified directly or through identifiers linked to the subjects.
- If the research does not involve prisoners as subjects.
- And, if the research is not FDA-regulated.

Although, the above research in fact qualifies as exempt from further IRB review, and has been identified as such, the Principal Investigator is responsible for notifying the IRB, in writing, of any changes that may have impact on the exempt status of this protocol. Such changes in the above research project cannot be initiated without prior IRB approval.

If you have any questions, please contact Camille Varacchi at Nemours Al duPont Hospital for Children 1600 Rockland Road, ARB-Room 291, Wilmington, Delaware 19803, 302-651-6807 or cvaracchi@nemours.org.

Please include your study title and reference number in all correspondence with this office.